

Efficient adiabatic connection approach for strongly correlated systems. Application to singlet-triplet gaps of biradicals

Daria Drwal,^{†,||} Pavel Beran,^{‡,¶,||} Michał Hapka,^{§,†} Marcin Modrzejewski,[§] Adam Sokół,[†] Libor Veis,^{*,‡} and Katarzyna Pernal^{*,†}

[†]*Institute of Physics, Lodz University of Technology,
ul. Wolczanska 219, 90-924 Lodz, Poland*

[‡]*J. Heyrovský Institute of Physical Chemistry, Academy of Sciences of the Czech Republic, v.v.i., Dolejškova 3, 18223 Prague 8, Czech Republic*

[¶]*Faculty of Mathematics and Physics, Charles University, Prague, Czech Republic*

[§]*Faculty of Chemistry, University of Warsaw, ul. L. Pasteura 1, 02-093 Warsaw, Poland*

^{||}*Contributed equally.*

E-mail: libor.veis@jh-inst.cas.cz; pernak@gmail.com

Abstract

Strong correlation can be essentially captured with multireference wavefunction methods such as complete active space self-consistent field (CASSCF) or density matrix renormalization group (DMRG). Still, an accurate description of the electronic structure of strongly correlated systems requires accounting for the dynamic electron correlation, which CASSCF and DMRG largely miss. In this work a new approach for the correlation energy based on the adiabatic connection (AC) is proposed. The AC_n method accounts for terms up to the desired order n in the coupling constant,

is rigorously size-consistent, free from instabilities and intruder states. It employs the particle-hole multireference random phase approximation and the Cholesky decomposition technique, which leads to a computational cost growing with the fifth power of the system size. Thanks to AC_n depending solely on one- and two-electron CAS reduced density matrix, the method is much more efficient than existing *ab initio* dynamic correlation methods for strong correlation. AC_n affords excellent results for singlet-triplet gaps of challenging organic biradicals. Development presented in this work opens new perspectives for accurate calculations of systems with dozens of strongly correlated electrons.

Electron correlation energy is defined with respect to the energy of a model (a reference) used to describe a given system. In other words, given a Hamiltonian \hat{H} , if Ψ^{ref} is the reference wavefunction and E^{ref} the corresponding energy i.e.

$$E^{\text{ref}} = \langle \Psi^{\text{ref}} | \hat{H} | \Psi^{\text{ref}} \rangle \quad , \quad (1)$$

then electron correlation comprises all electron interaction effects not accounted for by the chosen model, and the correlation energy pertains to the energy error

$$E_{\text{corr}} \equiv E_{\text{exact}} - E^{\text{ref}} \quad , \quad (2)$$

computed with respect to the exact energy E_{exact} (an eigenvalue of the Hamiltonian \hat{H}). Strongly correlated molecular systems require model wavefunctions consisting of multiple configurations to capture static correlation effects. The complete active space (CAS) method assumes selecting a number of (active) electrons and orbitals crucial for the static correlation and performing exact diagonalization in the active orbital subspace.^{1,2} The CAS model is a base of CASSCF-wavefunction and is frequently employed also in density matrix renormalization group (DMRG) calculations. The DMRG method is one of the most promising tools for strongly-correlated molecules³⁻⁷ due to its favourable scaling, which enables handling

of much more extensive active spaces than CASSCF allows. The reference energy, E^{ref} in Eq. (1), of all CAS-based methods does not include a substantial portion of electron correlation, called dynamic correlation, E_{corr} in Eq. (2). Even inclusion of dozens of orbitals in the active space is not sufficient to achieve a reliable description and the necessity to recover dynamic correlation remains the major challenge of DMRG.⁶ Although there exists many post-CAS methods aimed at including dynamic correlation, see e.g. Ref. 7, none is satisfactory due to the limitations both in accuracy and efficiency. In particular, perturbation theory-based approximations may suffer from the lack of size-consistency, intruder states, or unbalanced treatment of closed- and open-shell systems, which must be cured by level-shifting.⁸ The limitation of PT2 when combined with DMRG is the high scaling with the number of active orbitals resulting from treatment of 3- and 4-electron reduced density matrices (RDMs). Efforts to reduce the cost of handling high-order RDMs in NEVPT2 are worth noticing. These include the stochastic strongly contracted scheme,^{9,10} employing the cumulant expansion¹¹ or pre-screening techniques.¹² However, the improved efficiency may come at a cost of additional intruder states.¹³

The goal of this work is to address the challenge of recovering dynamic correlation and proposing an efficient and reliable computational method applicable to large active spaces. The presented approach builds upon the adiabatic connection formalism first introduced in the framework of Kohn-Sham DFT¹⁴⁻¹⁷ and recently formulated for CAS models.^{18,19}

Although the following discussion will pertain to a ground state energy, the presented formalism is general and can be directly applied to higher states. Derivation of the formula for the correlation energy in the adiabatic connection (AC) formalism begins with assuming a model Hamiltonian $\hat{H}^{(0)}$ (typically electron-electron interaction is either reduced or removed from $\hat{H}^{(0)}$), such that the reference function Ψ^{ref} is its eigenfunction

$$\hat{H}^{(0)} |\Psi^{\text{ref}}\rangle = E^{(0)} |\Psi^{\text{ref}}\rangle \quad . \quad (3)$$

The AC Hamiltonian \hat{H}^α is introduced as a combination of $\hat{H}^{(0)}$ and a scaled complementary operator \hat{H}'

$$\forall_{\alpha \in [0,1]} \quad \hat{H}^\alpha = \hat{H}^{(0)} + \alpha \hat{H}' \quad (4)$$

$$\hat{H}' = \hat{H} - \hat{H}^{(0)} \quad , \quad (5)$$

The eigenequation for \hat{H}^α reads

$$\hat{H}^\alpha |\Psi_\nu^\alpha\rangle = E_\nu^\alpha |\Psi_\nu^\alpha\rangle \quad . \quad (6)$$

where index ν pertains to the ν -th electronic state. The role of the coupling parameter α is to adiabatically turn on full electron correlation by varying α from 0 to 1. Namely, at $\alpha = 0$ electron interaction is reduced according to the assumed $\hat{H}^{(0)}$ model and the reference wavefunction is obtained as Ψ_0^α

$$|\Psi_0^{\alpha=0}\rangle = |\Psi^{\text{ref}}\rangle \quad . \quad (7)$$

The $\alpha = 1$ limit corresponds to electrons interacting at their full strength, so that both the exact energy and wavefunction are obtained

$$E_0^{\alpha=1} = E^{\text{exact}} \quad , \quad (8)$$

$$|\Psi_0^{\alpha=1}\rangle = |\Psi^{\text{exact}}\rangle \quad . \quad (9)$$

Exploiting the Hellmann-Feynman theorem $\frac{\partial E_0^\alpha}{\partial \alpha} = \langle \Psi_0^\alpha | \hat{H}' | \Psi_0^\alpha \rangle$, satisfied for $\alpha \in [0, 1]$, it is straightforward to show that the correlation energy, Eq.(2), is given exactly as

$$E_{\text{corr}} = \int_0^1 \left(\langle \Psi_0^\alpha | \hat{H}' | \Psi_0^\alpha \rangle - \langle \Psi^{\text{ref}} | \hat{H}' | \Psi^{\text{ref}} \rangle \right) d\alpha \quad . \quad (10)$$

The choice for the $\hat{H}^{(0)}$ Hamiltonian depends on the reference wavefunction. Our interest is in multireference CAS-based models which assume partitioning orbitals into sets of inac-

tive (fully occupied), active (fractionally occupied) and virtual (unoccupied) orbitals and constructing Ψ^{ref} as an antisymmetrized product of a single determinant comprising inactive orbitals and a multiconfigurational function utilizing active orbitals. Thus, we represent $\hat{H}^{(0)}$ as a sum of group Hamiltonians \hat{H}_I ^{18,20}

$$\hat{H}^{(0)} = \sum_I \hat{H}_I \quad (11)$$

where I corresponds to inactive, active or virtual group and \hat{H}_I consists of one- and two-particle operators

$$\hat{H}_I = \sum_{pq \in I} h_{pq}^{\text{eff}} \hat{a}_p^\dagger \hat{a}_q + \frac{1}{2} \sum_{pqrs \in I} \hat{a}_r^\dagger \hat{a}_s^\dagger \hat{a}_q \hat{a}_p \langle rs|pq \rangle \quad (12)$$

$$\forall_{pq \in I} \quad h_{pq}^{\text{eff}} = h_{pq} + \sum_{J \neq I} \sum_{r \in J} n_r [\langle pr|qr \rangle - \langle pr|rq \rangle] \quad (13)$$

Notice that $\langle rs|pq \rangle$ denotes a two-electron integral in the $x_1 x_2 x_1 x_2$ convention, and the effective one-electron Hamiltonian h^{eff} is a sum of kinetic and electron-nuclei operators, and the self-consistent field interaction of orbitals in a group I with the other groups [see the second term in Eq.(13)]. Throughout the paper it is assumed that indices p, q, r, s denote natural spinorbitals of the reference ($\alpha = 0$) model and $\{n_p\}$ are the corresponding natural occupation numbers. For this choice of $\hat{H}^{(0)}$, the α -dependent integrand in the correlation energy expression, Eq. (10), includes, among others, one electron terms depending on the difference between 1-RDM at $\alpha = 1$ and the reference one, $\gamma^\alpha - \gamma^{\alpha=0} = \gamma^\alpha - \gamma^{\text{ref}}$. Such terms are set to 0, under the assumption that for the properly chosen multireference wavefunction for a strongly correlated system, variation of γ^α with α can be ignored.

As it has been shown in Refs. 18,19, see also the Supporting Information (SI), choosing $\hat{H}^{(0)}$ as a group Hamiltonian and assuming that the 1-RDM stays constant with α , turn

Eq. (10) into the following AC correlation energy expression

$$E_{\text{corr}}^{\text{AC}} = \frac{1}{2} \sum'_{pqrs} \left(\int_0^1 \sum_{\nu \neq 0} \gamma_{pr}^{\alpha, 0\nu} \gamma_{qs}^{\alpha, \nu 0} d\alpha - \sum_{\nu \neq 0} \gamma_{pr}^{\alpha=0, 0\nu} \gamma_{qs}^{\alpha=0, \nu 0} \right) \langle rs|pq \rangle \quad , \quad (14)$$

where $\gamma^{0\nu, \alpha}$ are one-electron transition reduced density matrices (1-TRDM)

$$\gamma_{pq}^{0\nu, \alpha} = \langle \Psi_0^\alpha | \hat{a}_q^\dagger \hat{a}_p | \Psi_\nu^\alpha \rangle \quad . \quad (15)$$

It is important to notice a prime in the AC formula in Eq.(14), which indicates that terms pertaining to $pqrs$ belonging to the same group are excluded. This implies that electron correlation already accounted for by the active-orbitals-component of the reference wavefunction is not doubly counted in $E_{\text{corr}}^{\text{AC}}$.

We now briefly recapitulate developments presented in our earlier works^{18,19,21,22} leading to approximate correlation energy methods called AC and AC0. To formulate a working expression for the AC correlation energy, we have used Rowe's equation of motion^{23,24} in the particle-hole RPA approximation, where the excitation operator \hat{O}_ν^\dagger generating a state ν , $\hat{O}_\nu^\dagger |0\rangle = |\nu\rangle$, is approximated by single excitation operators as $\hat{O}_\nu^\dagger = \sum_{p>q} (X_{pq} \hat{a}_p^\dagger \hat{a}_q + Y_{pq} \hat{a}_q^\dagger \hat{a}_p)$. To distinguish this approximation from the conventional RPA,^{23,25-27} which assumes a single determinant as a reference, we called the ph-RPA equations

$$\begin{pmatrix} \mathcal{A}_-^\alpha & 0 \\ 0 & \mathcal{A}_+^\alpha \end{pmatrix} \begin{pmatrix} \tilde{\mathbf{Y}}_\nu^\alpha \\ \tilde{\mathbf{X}}_\nu^\alpha \end{pmatrix} = \omega_\nu^\alpha \begin{pmatrix} \mathbf{0} & \mathbf{1} \\ \mathbf{1} & \mathbf{0} \end{pmatrix} \begin{pmatrix} \tilde{\mathbf{Y}}_\nu^\alpha \\ \tilde{\mathbf{X}}_\nu^\alpha \end{pmatrix} \quad , \quad (16)$$

which are introduced for a general, multiconfigurational reference, the extended RPA (ERPA).^{24,28}

The ERPA equations have been written for the AC Hamiltonian, see Eq. (4), assuming the 1- and 2-RDM reference density matrices, leading to \mathcal{A}_\pm^α defined as

$$\forall_{\substack{p>q \\ r>s}} [\mathcal{A}_\pm^\alpha]_{pq,rs} = \frac{\langle \Psi^{\text{ref}} | [[\hat{a}_p^\dagger \hat{a}_q, [\hat{H}^\alpha, \hat{a}_s^\dagger \hat{a}_r]] \pm [\hat{a}_p^\dagger \hat{a}_q, [\hat{H}^\alpha, \hat{a}_r^\dagger \hat{a}_s]] | \Psi^{\text{ref}} \rangle}{(n_p - n_q)(n_r - n_s)} \quad , \quad (17)$$

Explicit expressions of $\mathcal{A}_{\pm}^{\alpha}$ in terms of 1- and 2-RDMs are presented in SI. Both \mathcal{A}_{+}^{α} and \mathcal{A}_{-}^{α} are symmetric and positive definite at $\alpha = 0$ and $\alpha = 1$ for the Hellmann-Feynman reference wavefunction Ψ^{ref} . Since the coupling constant dependence is passed to ERPA equations only via AC Hamiltonian \hat{H}^{α} , the matrices $\mathcal{A}_{\pm}^{\alpha}$ are linear in α , i.e.

$$\mathcal{A}_{\pm}^{\alpha} = \mathcal{A}_{\pm}^{(0)} + \alpha \mathcal{A}_{\pm}^{(1)} \quad . \quad (18)$$

In the ERPA model,²⁹ the α -dependent 1-TRDMs, Eq. (15), are given by the eigenvectors $\tilde{\mathbf{Y}}_{\nu}^{\alpha}$ as $\forall_{p>q} \left(n_p^{1/2} + n_q^{1/2} \right) \left[\tilde{\mathbf{Y}}_{\nu}^{\alpha} \right]_{pq} = \gamma_{qp}^{\alpha,0\nu} + \gamma_{pq}^{\alpha,0\nu}$, which allows one to turn Eq. (14) into a spin-free formula²¹

$$E_{\text{corr}}^{\text{AC}} = 2 \sum'_{\substack{p>q \\ r>s}} (n_p^{1/2} + n_q^{1/2})(n_r^{1/2} + n_s^{1/2}) \left(\int_0^1 \sum_{\nu} \left[\tilde{\mathbf{Y}}_{\nu}^{\alpha} \right]_{pq} \left[\tilde{\mathbf{Y}}_{\nu}^{\alpha} \right]_{rs} d\alpha - \left[\tilde{\mathbf{Y}}_{\nu}^{(0)} \right]_{pq} \left[\tilde{\mathbf{Y}}_{\nu}^{(0)} \right]_{rs} \right) \langle pr | qs \rangle \quad , \quad (19)$$

where $\tilde{\mathbf{Y}}_{\nu}^{(0)} = \tilde{\mathbf{Y}}_{\nu}^{\alpha=0}$. Eqs. (16) and (19) form ground for practical correlation energy calculation. This, however, requires solving the ERPA problem which formally scales with the 6th power of the system size. In addition, using the reference wavefunction in which the choice of the active orbitals is not optimal could lead to developing instability in the ERPA problem, for $\alpha \gg 0$.²¹ To lower the computational cost and avoid potential instabilities, we introduced an AC0 variant, assuming linearization of the integrand in Eq. (19), namely using $\tilde{\mathbf{Y}}_{\nu}^{\alpha} = \tilde{\mathbf{Y}}_{\nu}^{(0)} + \tilde{\mathbf{Y}}_{\nu}^{(1)}\alpha$, keeping the linear terms in α and carrying out the α integration,²¹

$$E_{\text{corr}}^{\text{AC0}} = 2 \sum'_{\substack{p>q \\ r>s}} (n_p^{1/2} + n_q^{1/2})(n_r^{1/2} + n_s^{1/2}) \sum_{\nu} \left[\tilde{\mathbf{Y}}_{\nu}^{(0)} \right]_{pq} \left[\tilde{\mathbf{Y}}_{\nu}^{(1)} \right]_{rs} \langle pr | qs \rangle \quad . \quad (20)$$

The low computational cost of AC0 stems from the fact that ERPA equations must be only solved at $\alpha = 0$ and for this value of the coupling constant the \mathcal{A}_{\pm} matrices are block diagonal. The largest block is of the dimension $N_{\text{act}}^2 \times N_{\text{act}}^2$ (N_{act} denotes a number of active orbitals), so the cost of its diagonalization is marginal even for dozens of active orbitals.

Despite the fact that encouraging results have been obtained with AC0 when combined with CASSCF^{21,22,30} or DMRG,³¹ α integration should in principle account for correlation more accurately than AC0. It is thus desirable to develop an AC method which on the one hand is exact in all orders of α , and on the other avoids solving the expensive ERPA problem. Ideally, such a method would be free of potential instabilities that might occur when α approaches 1. A novel AC method satisfying all the requirements is presented in this work.

Let us use the integral identity $\forall_{\text{Re}a>0} \quad 2a/\pi \int_0^\infty (\omega^2 + a^2)^{-1} d\omega = 1$ to express the AC correlation energy by means of the α -dependent dynamic density-density response matrix.³² This can be attained by employing the relations

$$\sum_\nu [\tilde{\mathbf{Y}}_\nu^\alpha]_{pq} [\tilde{\mathbf{Y}}_\nu^\alpha]_{rs} = \frac{2}{\pi} \int_0^\infty d\omega \sum_\nu [\tilde{\mathbf{Y}}_\nu^\alpha]_{pq} [\tilde{\mathbf{Y}}_\nu^\alpha]_{rs} \frac{\omega_\nu^\alpha}{\omega^2 + (\omega_\nu^\alpha)^2} \equiv \frac{1}{\pi} \int_0^\infty d\omega [\mathbf{C}^\alpha(\omega)]_{pq,rs} \quad (21)$$

in Eq.(19) which results in the formula

$$E_{\text{corr}}^{\text{AC}} = \frac{2}{\pi} \int_0^1 d\alpha \int_0^\infty d\omega \text{Tr} \left\{ [\mathbf{C}^\alpha(\omega) - \mathbf{C}^{\alpha=0}(\omega)]' \mathbf{g} \right\} \quad , \quad (22)$$

where

$$\forall_{\substack{p>q \\ r>s}} g_{pq,rs} = (n_p^{1/2} + n_q^{1/2})(n_r^{1/2} + n_s^{1/2}) \langle pr|qs \rangle \quad , \quad (23)$$

and the prime in Eq.(22) indicates that when taking a product of the matrices \mathbf{C} and \mathbf{g} terms $pqrs \in \text{active}$ are excluded. By using spectral representations of the matrices \mathcal{A}_+^α and \mathcal{A}_-^α in terms of the ERPA eigenvectors,³³ it is straightforward to show that the dynamic linear response matrix $\mathbf{C}^\alpha(\omega)$ follows from the linear equation given as (see SI for details)

$$[\mathcal{A}_+^\alpha \mathcal{A}_-^\alpha + \omega^2 \mathbf{1}] \mathbf{C}^\alpha(\omega) = \mathcal{A}_+^\alpha \quad . \quad (24)$$

To reduce the computational cost of solving Eq. (24), we introduce a decomposition of the

modified two-electron integrals \mathbf{g}

$$g_{pq,rs} = \sum_{L=1}^{N_{\text{Chol}}} D_{pq,L} D_{rs,L} \quad , \quad (25)$$

where $D_{pq,L}$ are the natural-orbital transformed Cholesky vectors of the Coulomb matrix multiplied by factors $n_p^{1/2} + n_q^{1/2}$, cf. Eq. (23). We expand $\mathbf{C}^\alpha(\omega)$ at $\alpha = 0$

$$\mathbf{C}^\alpha(\omega) = \sum_{n=0} \frac{1}{n!} \mathbf{C}(\omega)^{(n)} \alpha^n \quad , \quad (26)$$

$$\mathbf{C}(\omega)^{(n)} = \left. \frac{\partial^n \mathbf{C}^\alpha(\omega)}{\partial \alpha^n} \right|_{\alpha=0} \quad , \quad (27)$$

and solve Eq. (24) iteratively in the reduced space, by retrieving, in the n th iteration, the n th-order correction $\mathbf{C}^{(n)}$ projected on the space spanned by N_{Chol} transformed Cholesky vectors $\{\mathbf{D}_L\}$. To account for the prime (exclusion of terms for all-active indices $pqrs$) in the AC correlation energy, Eq. (22), define the auxiliary matrices of the transformed Cholesky vectors as

$$\forall_{p>q} \quad D_{pq,L}^1 = \begin{cases} 2D_{pq,L} & \text{if } pq \in \text{active} \\ D_{pq,L} & \text{otherwise} \end{cases} \quad , \quad (28)$$

$$\forall_{p>q} \quad D_{pq,L}^2 = \begin{cases} 0 & \text{if } pq \in \text{active} \\ D_{pq,L} & \text{otherwise} \end{cases} \quad . \quad (29)$$

Assuming expansion of the response matrix $\mathbf{C}^\alpha(\omega)$, cf. Eq. (26), up to n th order in α , and employing Cholesky decomposition of integrals, Eq. (25) together with the matrices \mathbf{D}^1 and \mathbf{D}^2 in Eq. (22) lead to a new AC formula for the correlation energy reading

$$E_{\text{corr}}^{\text{AC}_n} = \frac{2}{\pi} \text{Tr} \left[\left(\int_0^\infty d\omega \sum_{k=1}^n \frac{\bar{\mathbf{C}}(\omega)^{(k)}}{k!(k+1)} \right) \mathbf{D}^2 \right] \quad . \quad (30)$$

The matrices $\bar{\mathbf{C}}(\omega)^{(n)}$ defined as

$$\bar{\mathbf{C}}(\omega)^{(n)} = \mathbf{C}(\omega)^{(n)} \mathbf{D}^1 \quad (31)$$

are of the dimension $M^2 \times N_{\text{Chol}}$, which is reduced comparing to the $M^2 \times M^2$ dimension of $\mathbf{C}(\omega)^{(n)}$, since by construction the number of Cholesky vectors is one order of magnitude smaller than M^2 , i.e. $N_{\text{Chol}} \sim M$. Employing the linearity in α of the matrices $\mathcal{A}_{\pm}^{\alpha}$, cf. Eq. (18) in Eq. (24), one finds the following recursive formula for the n th-order term $\bar{\mathbf{C}}(\omega)^{(n)}$

$$\bar{\mathbf{C}}(\omega)^{(0)} = \bar{\mathbf{A}}_+^{(0)} \mathbf{D}^1 \quad (32)$$

$$\bar{\mathbf{C}}(\omega)^{(1)} = \bar{\mathbf{A}}_+^{(1)} \mathbf{D}^1 - \bar{\mathbf{A}}^{(1)} \bar{\mathbf{C}}(\omega)^{(0)} \quad (33)$$

$$\forall_{n \geq 2} \quad \bar{\mathbf{C}}(\omega)^{(n)} = -n \bar{\mathbf{A}}^{(1)} \bar{\mathbf{C}}(\omega)^{(n-1)} - n(n-1) \bar{\mathbf{A}}^{(2)} \bar{\mathbf{C}}(\omega)^{(n-2)} \quad (34)$$

where the required matrices are given by the ERPA matrices $\mathcal{A}_{\pm}^{(0)}$ and $\mathcal{A}_{\pm}^{(1)}$ (see SI for their explicit forms in terms of 1-, 2-RDMs)

$$\bar{\mathbf{A}}_+^{(0)} = \Lambda(\omega) \mathcal{A}_+^{(0)} \quad , \quad (35)$$

$$\bar{\mathbf{A}}_+^{(1)} = \Lambda(\omega) \mathcal{A}_+^{(1)} \quad , \quad (36)$$

$$\bar{\mathbf{A}}^{(1)} = \Lambda(\omega) \left(\mathcal{A}_+^{(0)} \mathcal{A}_-^{(1)} + \mathcal{A}_+^{(1)} \mathcal{A}_-^{(0)} \right) \quad , \quad (37)$$

$$\bar{\mathbf{A}}^{(2)} = \Lambda(\omega) \mathcal{A}_+^{(1)} \mathcal{A}_-^{(1)} \quad , \quad (38)$$

$$\Lambda(\omega) = \left(\mathcal{A}_+^{(0)} \mathcal{A}_-^{(0)} + \omega^2 \mathbf{1} \right)^{-1} \quad . \quad (39)$$

The correlation energy expression in Eq. (30) together with the recursive relation in Eqs. (32)-(34) is the central achievement of this work. It allows one to compute the correlation energy for strongly correlated systems at the cost scaling with only the 5th power of the system size. All matrix operations scale as $M^4 N_{\text{Chol}}$ down from M^6 scaling of the original ERPA problem in Eq. (16). Notice that the cost of computing the $\Lambda(\omega)$ matrix is

marginal, since the inverted matrix is block diagonal with the largest block of the dimension $N_{\text{act}}^2 \times N_{\text{act}}^2$.

By setting the maximum order of expansion of the response matrix $\mathbf{C}(\omega)$ in Eq. (30) to 1, the correlation energy AC_n becomes equivalent to the AC0 approximation, cf. Eq. (20). In the limit $n \rightarrow \infty$, $E_{\text{corr}}^{\text{AC}_n}$ value approaches the AC energy given according to the formula in Eq. (19), if the Taylor series is convergent. Numerically this equality requires a sufficient accuracy both in the frequency integration and in the Cholesky decomposition of two-electron integrals.

Going beyond the 1st-order terms in the coupling constant is potentially beneficial, since higher-orders gain importance as α approaches 1. Higher-order contributions are effectively maximized if the AC integrand W^α in Eq. (22), $W^\alpha = \int_0^\infty d\omega \text{Tr} \{[\mathbf{C}^\alpha(\omega) - \mathbf{C}^{\alpha=0}(\omega)]' \mathbf{g}\}$, is linearly extrapolated from $W^{\alpha=1}$ to the exact limit $W^{\alpha=0} = 0$. Such an extrapolation method leading to the approximation $E_{\text{corr}}^{\text{AC}} = \frac{2}{\pi} \int_0^1 \alpha W^{\alpha=1} d\alpha$ has already been proposed in Ref. 18. If it is used together with the formula in Eq.(22), the expansion shown in Eq.(26) and the Cholesky decomposition of two-electron integrals, one obtains the formula

$$E_{\text{corr}}^{\text{AC}_{1n}} = \frac{1}{\pi} \text{Tr} \left[\left(\int_0^\infty d\omega \sum_{k=1}^n \frac{\bar{\mathbf{C}}(\omega)^{(k)}}{k!} \right) \mathbf{D}^2 \right] , \quad (40)$$

which will be denoted as AC_{1n} . Notice that in the frequency integrated k th-order term in Eq. (40) contributes to the correlation energy by the factor $(k+1)/2$ greater than its counterpart in the expression given in Eq. (30).

The Cholesky decomposition of the Coulomb integrals matrix in the AO basis was carried out using a modified program originally used in Refs. 34,35. The implementation was done according to Ref. 36. The Cholesky vectors in the AO basis, $R_{pq,L}$, were generated until the satisfaction of the trace condition $\sum_{p \geq q} (\langle pp|qq \rangle - \sum_L R_{pq,L} R_{pq,L}) < 10^{-2}$. The convergence threshold was previously tested as a part of the default set of numerical thresholds in Table 1 of Ref. 34.

For the ω integration in the AC_n correlation energy, we have used a modified Gauss–Legendre quadrature as described in Ref. 37. With the 18-point grid, the accuracy of the absolute value of energy achieves 10^{-2} mHa, which results in 10^{-2} eV accuracy in the singlet-triplet gaps.

To assess the accuracy of the AC_n approaches, we have applied them to two benchmark datasets of singlet-triplet (ST) energy gaps: the single-reference systems set of Schreiber et al.³⁸ and multi-reference organic biradicals studied by Stoneburner et al.³⁹ In the single-reference dataset we employed the TZVP⁴⁰ basis set and compared our data against the CC3³⁸ results. The aug-cc-pVTZ basis and doubly electron-attached (DEA) equation-of-motion (EOM) coupled-cluster (CC) 4-particle–2-hole (4p-2h) reference³⁹ were used for the biradicals. All CASSCF calculations were performed in the Molpro⁴¹ program. All AC methods were implemented in the GammCor program.⁴²

Computing the correlation energy with the AC_n method requires either fixing the maximum order of expansion with respect to the coupling constant, n in Eq.(30), or continuing the expansion until a prescribed convergence threshold is met. The advantage of the former strategy is that size-consistency is strictly preserved. For each system we found that the AC_n correlation energy converges with n for the chosen active space. A typical convergence behavior for the singlet, triplet and ST energies is presented in Figure 1. It can be seen that already for $n=3$ the AC_n ST gap deviates by only 0.01 eV from the AC value, computed using Eq. (19). For all other biradicals and single-reference systems we found that setting $n = 10$ in Eq.(30) is sufficient to converge ST gaps within 10^{-2} eV, thus, $n = 10$ has been set for all systems.

In Table 1 we present ST gaps for the subset of Ref. 38 dataset. The CASSCF method predicts too narrow ST gaps with the mean error approaching -0.4 eV, which results from the unbalanced treatment of closed-shell singlet and open-shell triplet states. The addition of correlation energy using adiabatic connection greatly reduces the errors. The mean unsigned error (MUE) of AC0 amounts to 0.24 eV. The performance is further improved by AC_n which

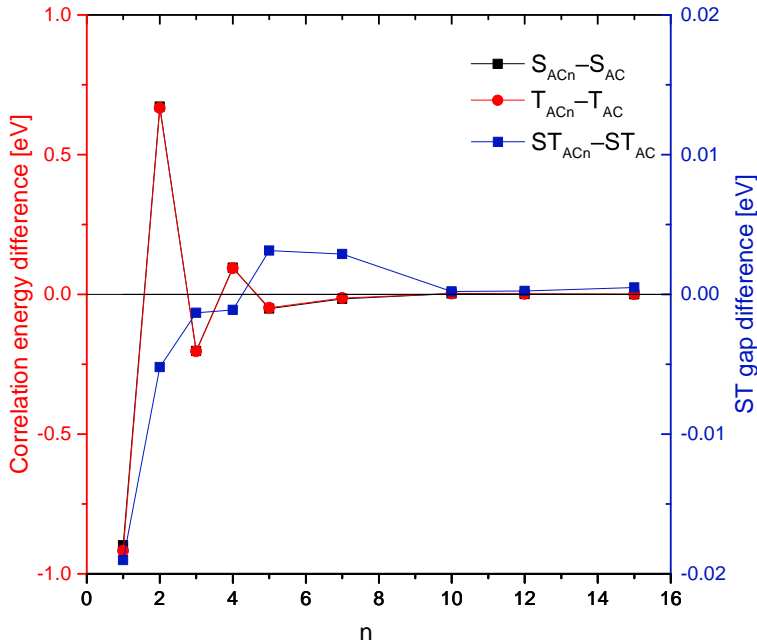


Figure 1: Differences of AC_n and AC correlation energies for singlet (S) and triplet (T) states (left axis) and ST gaps (right axis) as a function of n for the $C_4H_2-1,3-(CH_2)_2$ biradical. Notice that black markers overlap with the red ones.

affords MUE of 0.13 eV. Maximizing the contribution from high-order terms in α , attained in AC_{1n} , leads to ST gaps of the same unsigned error as that of AC_n . Noticeable, the signed error is reduced, which indicates that higher order terms play more important role for open-shell than for the closed-shell states. The accuracy of AC_n is on a par with NEVPT2 and only slightly worse than best CASPT2 estimations from Ref. 38. The standard deviation of AC_0 , amounting to 0.23 eV, is reduced to 0.11 eV by AC_n , which parallels the standard deviation of the perturbation methods.

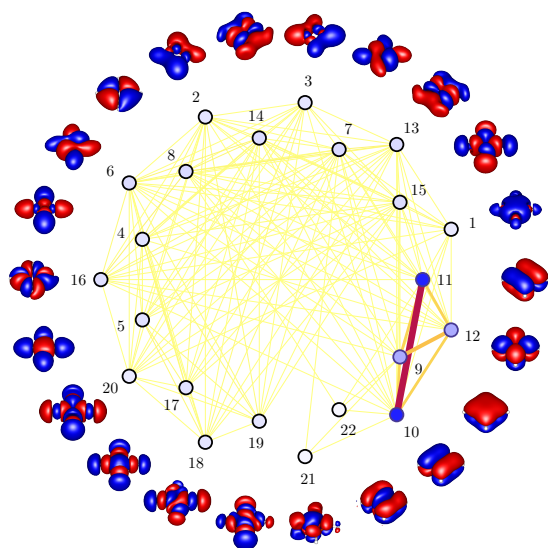
In Ref. 39 a systematic design of active spaces for biradicals based on the correlated participating orbital (CPO) scheme⁴⁴ was presented. Here, we take a different approach and identify the most appropriate CASs by means of single-orbital entropies and two-orbital mutual information.^{45–47}

Figure 2 shows the correlation measures for singlet and triplet states of prototypical biradicals, C_4H_4 and $C_5H_5^+$, obtained with, respectively, CAS(20,22) and CAS(14,16) active spaces (cf. description in SI). We observe that the π orbitals of C_4H_4 and $C_5H_5^+$ are well

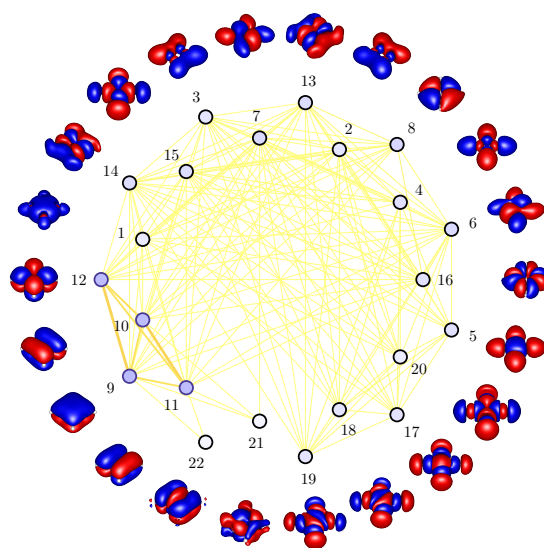
Table 1: ST gaps ($E_T - E_S$), mean errors (ME), mean unsigned errors (MUE), and standard deviations (Std. Dev.) computed with respect to CC3 reference data. All values in eV.

Molecule	T state	CASSCF ^a	AC1 _n	AC _n	AC0	NEVPT2 ^b	CASPT2 ^c	CC3 ^c
Ethene	1 ³ B _{1u}	3.78	4.53	4.56	4.69	4.60	4.60	4.48
E-butadiene	1 ³ B _u	2.77	3.44	3.43	3.46	3.38	3.34	3.32
All-E-hexatriene	1 ³ A _g	2.66	2.83	2.81	2.80	2.73	2.71	2.69
All-E-octatetraene	1 ³ B _u	2.25	2.46	2.43	2.39	2.32	2.33	2.30
Cyclopropene	1 ³ B ₂	3.78	4.42	4.44	4.56	4.56	4.35	4.34
Cyclopentadiene	1 ³ B ₂	2.75	3.34	3.34	3.37	3.32	3.28	3.25
Norbornadiene	1 ³ A ₂	3.07	3.92	3.89	3.86	3.79	3.75	3.72
Benzene	1 ³ B _{1u}	3.74	4.17	4.21	4.37	4.32	4.17	4.12
Naphthalene	1 ³ B _{2u}	2.93	3.19	3.21	3.29	3.26	3.20	3.11
Furan	1 ³ B ₂	3.54	4.09	4.16	4.30	4.33	4.17	4.48
Pyrrole	1 ³ B ₂	3.95	4.47	4.52	4.67	4.73	4.52	4.48
Imidazole	1 ³ A'	4.42	4.70	4.74	4.85	4.77	4.65	4.69
Pyridine	1 ³ A ₁	3.81	4.28	4.34	4.53	4.47	4.27	4.25
s-Tetrazine	1 ³ B _{3u}	2.43	2.27	2.05	1.51	1.64	1.56	1.89
Formaldehyde	1 ³ A ₂	3.32	3.80	3.74	3.77	3.75	3.58	3.55
Acetone	1 ³ A ₂	4.17	4.27	4.29	4.90	4.10	4.08	4.05
Formamide	1 ³ A''	4.72	5.31	5.47	5.60	5.64	5.40	5.36
Acetamide	1 ³ A''	4.77	5.46	5.57	5.73	5.52	5.53	5.42
Propanamide	1 ³ A''	4.79	5.51	5.61	5.80	5.54	5.44	5.45
ME		-0.38	0.08	0.10	0.18	0.10	0.00	-
MUE		0.45	0.13	0.13	0.24	0.14	0.07	-
Std. Dev.		0.35	0.15	0.11	0.23	0.13	0.12	-

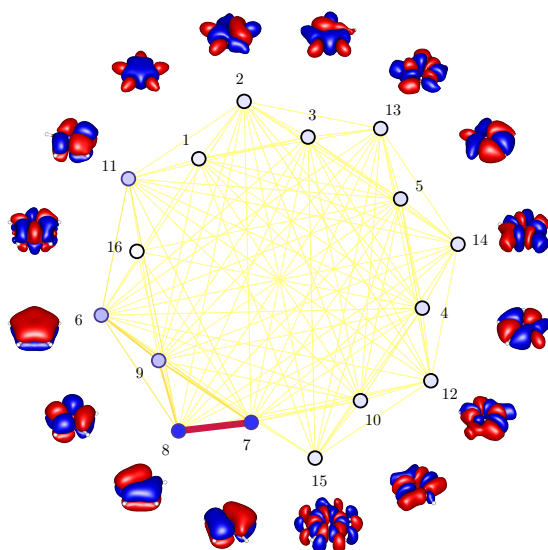
^a active spaces from Ref. 38 ^b results from Ref. 43 ^c results from Ref. 38



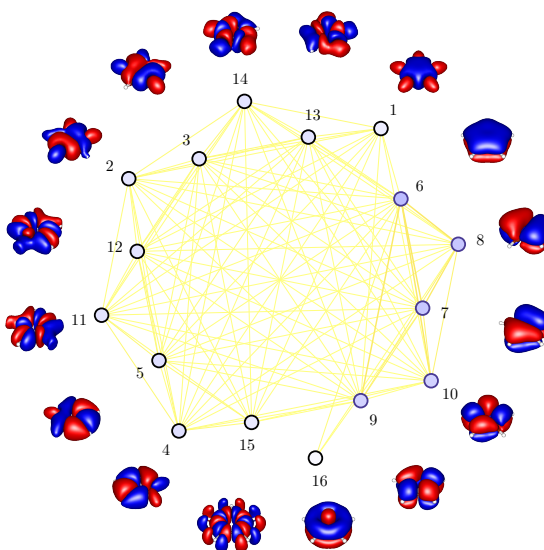
(a) C_4H_4 , singlet state, CAS(20,22)



(b) C_4H_4 , triplet state, CAS(20,22)



(c) $C_5H_5^+$, singlet state, CAS(14,16)



(d) $C_5H_5^+$, triplet state, CAS(14,16)



(e) Scales used for visualizing of correlations

Figure 2: The DMRG mutual information (colored edges) and single-orbital entropies (colored vertices) of C_4H_4 and $C_5H_5^+$ for the lowest singlet and triplet states. Numbers in the graphs correspond to indices of the DMRG-SCF (C_4H_4) and CASSCF ($C_5H_5^+$) natural orbitals presented together with their occupation numbers in SI. Blue circles represent the π orbitals with $s_i > 0.19$.

separated from the others in terms of their single-orbital entropies ($s_i > 0.19$, see SI) and represent a natural choice of the active space selection. The largest values of s_i correspond to the singly occupied frontier orbitals in the singlet states. These orbital pairs also possess the largest values of mutual information, which stems from a strong correlation of the frontier orbitals due to the singlet type coupling of these open shells. Notice that both single-orbital entropies and mutual information of the singly occupied orbitals are much lower in the case of the triplet states. This is due to the fact that the triplet states were calculated as high-spin projections and thus can be qualitatively described with a single determinant. When analyzing the triplet states, one can however see that all the π orbitals have similar values of their single-orbital entropies and that e.g. CAS(2,4) (nCPO active space in Ref. 39) is not a reasonable choice. In fact, for this imbalanced active space, we have experienced divergence of the AC_n series, see the last entry of Table 1 in SI.

Table 2: ST gaps ($E_T - E_S$) in eV and errors with respect to DEA-EOMCC[4p-2h]³⁹ (ref.) predictions. Labels: 1 – C₄H₄, 2 – C₅H₅⁺, 3 – C₄H₃NH₂, 4 – C₄H₃CHO, 5 – C₄H₂NH₂(CHO), 6 – C₄H₂-1,2-(CH₂)₂, 7 – C₄H₂-1,3-(CH₂)₂.

sys.	CASSCF	AC1 _n	AC _n	AC0	ftPBE ^a	RASPT2 ^b	ref.
1	0.44	0.18	0.13	0.00	0.11	0.19	0.18
2	-0.70	-0.71	-0.77	-0.86	-0.64	-0.65	-0.60
3	0.39	0.12	0.07	-0.08	0.03	0.11	0.12
4	0.41	0.17	0.12	-0.02	0.09	0.16	0.16
5	0.60	0.39	0.37	0.14	0.45	0.32	0.25
6	3.33	3.44	3.44	3.46	3.34	3.27	3.37
7	-0.92	-0.89	-0.90	-0.92	-0.66	-0.80	-0.80
ME	0.13	0.00	-0.03	-0.14	0.01	-0.01	-
MUE	0.20	0.06	0.08	0.16	0.09	0.04	-
MU%E	102.3	13.7	26.1	69.6	37.6	7.2	-
Std. Dev.	0.20	0.09	0.10	0.11	0.12	0.05	-

^a ftPBE results taken from Ref. 48

^b RASPT2 (valence- π , π CPO active space) results taken from Ref. 39

The analysis of mutual information and single-orbital entropies of prototypical biradicals have allowed us to define optimal active spaces: CAS(4,4) for C₄H₄, C₄H₃NH₂, C₄H₃CHO, C₄H₂NH₂(CHO), CAS(4,5) for C₅H₅⁺, and CAS(6,6) for C₄H₂-1,2-(CH₂)₂, and C₄H₂-1,3-

(CH₂)₂. The choice of the orbitals in CAS is therefore such that all valence π orbitals on or adjacent to the carbon ring are included and only the mostly correlated orbitals, of the occupancies in the range (0.05, 1.95), enter the active space. The chosen active spaces are close to the π CPO scheme considered in Ref. 39, with the difference that nearly unoccupied orbitals included in π CPO, shown to be uncorrelated according to our mutual information analysis, are excluded.

Similar to the single-reference case, the performance of the CASSCF method for the ST gaps in biradicals is seriously affected by the lack of dynamic correlation (Table 2). Even though the CASSCF gaps of three systems (C₅H₅⁺, 1,2- and 1,3-isomers) are in error of only 0.1 eV, the overall MUE is as large as 0.20 eV and the mean average unsigned percentage error (MU%E) exceeds 100%. The AC0 method overcompensates the errors of CASSCF. For biradicals 1, 3, 4, the excessive reduction of the ST gaps by AC0 results in a wrong ordering of states. Both AC_n and AC1_n approaches capture correlation in high orders of α and greatly improve over AC0. The ordering of states is correct and the average error falls below 0.10 eV as compared to the 0.16 eV error of AC0. AC1_n performs slightly better than AC_n in terms of MUEs, the errors are 0.06 eV and 0.08 eV, respectively, and significantly better in terms of percentage errors. The improved MU%E of AC1_n (14% vs. 26%) is due to the good performance of this method for small gaps (systems 1, 3, and 4). These excellent results imply a crucial role of the high-order terms in AC which should enter the correlation energy with high weights.

Table 2 includes the ftPBE results from Ref. 48. The latter method performs better than other MC-PDFT⁴⁹ approaches for ST gaps of biradicals. Similarly to AC approximations, MC-PDFT is a post-CASSCF method relying on only 1- and 2-RDMs obtained from CAS. It employs density functional exchange-correlation functionals with modified arguments to describe electron correlation. As shown in Table 2, the accuracy of ST gaps predictions by ftPBE does not match that of the AC1_n method, with the percentage error nearly tripled and amounting to 38%. Comparing the computational efficiency of the adiabatic connection

and MC-PDFT approximations, AC_n (or $AC1_n$) formally scale with the 5th power of the system-size which is one order more than scaling of MC-PDFT (timings of both methods are presented in SI). It should be noticed, however, that in the case of both AC_n and MC-PDFT the major share of the total computational time is spent on CASSCF calculation.

The accuracy achieved by $AC1_n$ comes close to that of the RASPT2 method. Comparison of RASPT2 (or CASPT2³⁹) results with those of AC_n requires some care. These perturbation methods involve parameters to remove intruder states and to compensate their tendency to underestimate gap energies between closed- and open-shell states.⁵⁰ The default value of the ionization potential-electron affinity shift⁸ used in Ref. 39 improves ST gaps of biradicals predicted by CASPT2 and RASPT2 methods. In general, however, the shift may be problematic for strongly correlated systems, e.g. complexes with transition metals, and their tuning may be required.^{51,52}

In summary, we have proposed a computational approach to the correlation energy in complete active space models. The novel AC_n formula for the correlation energy is based on a systematic expansion with respect to the adiabatic connection coupling constant α . Application to singlet-triplet gaps of single- and multi-reference systems revealed the need to account for higher-order terms in the α -expansion. The $AC_n/AC1_n$ approaches showed a systematic improvement over the first-order $AC0$ method. The $AC1_n$ variant, which maximizes contributions from the high-order terms, was identified as the best-performing AC approximation. Owing to the Cholesky decomposition technique the AC_n methods achieve $\mathcal{O}(N^5)$ scaling of the computational time with the system size. Since they involve only 1- and 2-RDMs, they are well-suited to treat large active spaces. Importantly, the formalism used to derive AC_n is not limited to a particular form of the model Hamiltonian $\hat{H}^{(0)}$, thus further improvements in accuracy could be achieved with models other than that assumed in this work.

Compared to other correlation energy methods for strong correlation, AC_n emerges as having the most favorable accuracy to cost ratio. Advantages of AC_n over perturbation

methods, such as CASPT2 or RASPT2, include not only the ability to treat dozens of active orbitals, but also the lack of parameters and strict size-consistency.⁵³ We believe that the presented development opens new perspectives for meeting the challenge of strong correlation, e.g., by DMRG⁶ methods.

Acknowledgment

This work was supported by the National Science Center of Poland under grant no. 2019/35/B/ST4/01310, the Charles University in Prague (grant no. CZ.02.2.69/0.0/0.0/19_073/0016935), the Ministry of Education, Youth and Sports of the Czech Republic through the e-INFRA CZ (ID:90140), and by the European Centre of Excellence in Exascale Computing TREX - Targeting Real Chemical Accuracy at the Exascale. This project has received funding from the European Union's Horizon 2020 - Research and Innovation program - under grant agreement no. 952165.

References

- (1) Roos, B. O. The complete active space self-consistent field method and its applications in electronic structure calculations. *Adv. Chem. Phys.* **1987**, *69*, 399.
- (2) Olsen, J. The CASSCF method: A perspective and commentary. *International Journal of Quantum Chemistry* **2011**, *111*, 3267–3272.
- (3) Chan, G. K.-L.; Sharma, S. The Density Matrix Renormalization Group in Quantum Chemistry. *Annu. Rev. Phys. Chem.* **2011**, *62*, 465–481.
- (4) Szalay, S.; Pfeffer, M.; Murg, V.; Barcza, G.; Verstraete, F.; Schneider, R.; Örs Legeza, Tensor product methods and entanglement optimization forab initioquantum chemistry. *Int. J. Quant. Chem.* **2015**, *115*, 1342–1391.

- (5) Olivares-Amaya, R.; Hu, W.; Nakatani, N.; Sharma, S.; Yang, J.; Chan, G. K.-L. The ab-initio density matrix renormalization group in practice. *The Journal of chemical physics* **2015**, *142*, 034102.
- (6) Baiardi, A.; Reiher, M. The density matrix renormalization group in chemistry and molecular physics: Recent developments and new challenges. *J. Chem. Phys.* **2020**, *152*, 040903.
- (7) Cheng, Y.; Xie, Z.; Ma, H. Post-Density Matrix Renormalization Group Methods for Describing Dynamic Electron Correlation with Large Active Spaces. *The Journal of Physical Chemistry Letters* **2022**, *13*, 904–915.
- (8) Roca-Sanjuán, D.; Aquilante, F.; Lindh, R. Multiconfiguration second-order perturbation theory approach to strong electron correlation in chemistry and photochemistry. *Wiley Interdiscip. Rev.: Comput. Mol. Sci.* **2012**, *2*, 585–603.
- (9) Mahajan, A.; Blunt, N. S.; Sabzevari, I.; Sharma, S. Multireference configuration interaction and perturbation theory without reduced density matrices. *J. Chem. Phys.* **2019**, *151*, 211102.
- (10) Blunt, N. S.; Mahajan, A.; Sharma, S. Efficient multireference perturbation theory without high-order reduced density matrices. *J. Chem. Phys.* **2020**, *153*, 164120.
- (11) Kurashige, Y.; Chalupský, J.; Lan, T. N.; Yanai, T. Complete active space second-order perturbation theory with cumulant approximation for extended active-space wavefunction from density matrix renormalization group. *The Journal of chemical physics* **2014**, *141*, 174111.
- (12) Guo, Y.; Sivalingam, K.; Neese, F. Approximations of density matrices in N-electron valence state second-order perturbation theory (NEVPT2). I. Revisiting the NEVPT2 construction. *The Journal of Chemical Physics* **2021**, *154*, 214111.

- (13) Guo, Y.; Sivalingam, K.; Kollmar, C.; Neese, F. Approximations of density matrices in N-electron valence state second-order perturbation theory (NEVPT2). II. The full rank NEVPT2 (FR-NEVPT2) formulation. *The Journal of Chemical Physics* **2021**, *154*, 214113.
- (14) Harris, J.; Jones, R. O. The surface energy of a bounded electron gas. *J. Phys. F: Met. Phys.* **1974**, *4*, 1170.
- (15) Langreth, D.; Perdew, J. Exchange-correlation energy of a metallic surface: Wave-vector analysis. *Phys. Rev. B* **1977**, *15*, 2884.
- (16) Gunnarsson, O.; Lundqvist, B. Exchange and correlation in atoms, molecules, and solids by the spin-density-functional formalism. *Phys. Rev. B* **1976**, *13*, 4274.
- (17) Teale, A. M.; Coriani, S.; Helgaker, T. Accurate calculation and modeling of the adiabatic connection in density functional theory. *J. Chem. Phys.* **2010**, *132*, 164115.
- (18) Pernal, K. Electron Correlation from the Adiabatic Connection for Multireference Wave Functions. *Phys. Rev. Lett.* **2018**, *120*, 013001.
- (19) Pernal, K. Exact and approximate adiabatic connection formulae for the correlation energy in multireference ground and excited states. *J. Chem. Phys.* **2018**, *149*, 204101.
- (20) Rosta, E.; Surján, P. Two-body zeroth order Hamiltonians in multireference perturbation theory: The APSG reference state. *J. Chem. Phys.* **2002**, *116*, 878.
- (21) Pastorczak, E.; Pernal, K. Correlation Energy from the Adiabatic Connection Formalism for Complete Active Space Wave Functions. *J. Chem. Theory Comput.* **2018**, *14*, 3493–3503.
- (22) Pastorczak, E.; Pernal, K. Electronic Excited States from the Adiabatic-Connection Formalism with Complete Active Space Wave Functions. *J. Phys. Chem. Lett.* **2018**, *9*, 5534–5538.

- (23) Rowe, D. J. Equations-of-Motion Method and the Extended Shell Model. *Rev. Mod. Phys.* **1968**, *40*, 153.
- (24) Chatterjee, K.; Pernal, K. Excitation energies from extended random phase approximation employed with approximate one-and two-electron reduced density matrices. *J. Chem. Phys.* **2012**, *137*, 204109.
- (25) Eshuis, H.; Bates, J.; Furche, F. Electron correlation methods based on the random phase approximation. *Theor. Chem. Acc.* **2012**, *131*, 1084.
- (26) Chen, G.; Voora, V.; Agee, M.; Balasubramani, S.; Furche, F. Random-phase approximation methods. *Annu. Rev. Phys. Chem.* **2017**, *68*, 19.
- (27) Ren, X.; Rinke, P.; Joas, C.; Scheffler, M. Random-phase approximation and its applications in computational chemistry and materials science. *J. Mater. Sci.* **2012**, *47*, 7447.
- (28) Pernal, K.; Chatterjee, K.; Kowalski, P. H. How accurate is the strongly orthogonal geminal theory in predicting excitation energies? Comparison of the extended random phase approximation and the linear response theory approaches. *J. Chem. Phys.* **2014**, *140*, 014101.
- (29) Pernal, K. Intergeminal Correction to the Antisymmetrized Product of Strongly Orthogonal Geminals Derived from the Extended Random Phase Approximation. *J. Chem. Theory Comput.* **2014**, *10*, 4332–4341.
- (30) Pastorczak, E.; Hapka, M.; Veis, L.; Pernal, K. Capturing the Dynamic Correlation for Arbitrary Spin-Symmetry CASSCF Reference with Adiabatic Connection Approaches: Insights into the Electronic Structure of the Tetramethyleneethane Diradical. *J. Phys. Chem. Lett.* **2019**, *10*, 4668–4674.

- (31) Beran, P.; Matoušek, M.; Hapka, M.; Pernal, K.; Veis, L. Density matrix renormalization group with dynamical correlation via adiabatic connection. *J. Chem. Theory Comput.* **2021**, *17*, 7575–7585.
- (32) Drwal, D.; Pastorzak, E.; Pernal, K. Excited states in the adiabatic connection fluctuation-dissipation theory: Recovering missing correlation energy from the negative part of the density response spectrum. *J. Chem. Phys.* **2021**, *154*, 164102.
- (33) Furche, F. On the density matrix based approach to time-dependent density functional response theory. *J. Chem. Phys.* **2001**, *114*, 5982–5992.
- (34) Modrzejewski, M.; Yourdkhani, S.; Klimeš, J. Random phase approximation applied to many-body noncovalent systems. *J. Chem. Theory Comput.* **2020**, *16*, 427–442.
- (35) Modrzejewski, M.; Yourdkhani, S.; Šmiga, S.; Klimeš, J. Random-Phase Approximation in Many-Body Noncovalent Systems: Methane in a Dodecahedral Water Cage. *J. Chem. Theory Comput.* **2021**, *17*, 804–817.
- (36) Aquilante, F.; Boman, L.; Bostrom, J.; Koch, H.; Lindh, R.; de Meras, A. S.; Pedersen, T. B. In *Linear-Scaling Techniques in Computational Chemistry and Physics: Methods and Applications*; Zalesny, R., Papadopoulos, M. G., Mezey, P. G., Leszczyński, J., Eds.; Springer Netherlands: Dordrecht, 2011; pp 301–343.
- (37) Ren, X.; Rinke, P.; Blum, V.; Wieferink, J.; Tkatchenko, A.; Sanfilippo, A.; Reuter, K.; Scheffler, M. Resolution-of-identity approach to Hartree–Fock, hybrid density functionals, RPA, MP2 and GW with numeric atom-centered orbital basis functions. *New J. Phys.* **2012**, *14*, 053020.
- (38) Schreiber, M.; Silva-Junior, M. R.; Sauer, S. P.; Thiel, W. Benchmarks for electronically excited states: CASPT2, CC2, CCSD, and CC3. *J. Chem. Phys.* **2008**, *128*, 134110.

- (39) Stoneburner, S. J.; Shen, J.; Ajala, A. O.; Piecuch, P.; Truhlar, D. G.; Gagliardi, L. Systematic design of active spaces for multi-reference calculations of singlet–triplet gaps of organic diradicals, with benchmarks against doubly electron-attached coupled-cluster data. *J. Chem. Phys.* **2017**, *147*, 164120.
- (40) Schäfer, A.; Horn, H.; Ahlrichs, R. Fully optimized contracted Gaussian basis sets for atoms Li to Kr. *J. Chem. Phys.* **1992**, *97*, 2571–2577.
- (41) Werner, H.-J.; Knowles, P. J.; Knizia, G.; Manby, F. R.; Schütz, M. Molpro: a general-purpose quantum chemistry program package. *Wiley Interdiscip. Rev.: Comput. Mol. Sci.* **2012**, *2*, 242–253.
- (42) Pernal, K.; Hapka, M.; Przybytek, M.; Modrzejewski, M.; Sokół, A. GammCor code. <https://github.com/pernalk/GAMMCOR>, 2022.
- (43) Schapiro, I.; Sivalingam, K.; Neese, F. Assessment of n -electron valence state perturbation theory for vertical excitation energies. *J. Chem. Theory Comput.* **2013**, *9*, 3567–3580.
- (44) Tishchenko, O.; Zheng, J.; Truhlar, D. G. Multireference Model Chemistries for Thermochemical Kinetics. *J. Chem. Theory Comput.* **2008**, *4*, 1208–1219.
- (45) Stein, C. J.; Reiher, M. Automated Selection of Active Orbital Spaces. *J. Chem. Theory Comput.* **2016**, *12*, 1760–1771.
- (46) Legeza, O.; Sólyom, J. Optimizing the density-matrix renormalization group method using quantum information entropy. *Phys. Rev. B* **2003**, *68*.
- (47) Golub, P.; Antalík, A.; Veis, L.; Brabec, J. Machine Learning-Assisted Selection of Active Spaces for Strongly Correlated Transition Metal Systems. *J. Chem. Theory Comput.* **2021**, *17*, 6053–6072.

- (48) Stoneburner, S. J.; Truhlar, D. G.; Gagliardi, L. MC-PDFT can calculate singlet–triplet splittings of organic diradicals. *J. Chem. Phys.* **2018**, *148*, 064108.
- (49) Li Manni, G.; Carlson, R. K.; Luo, S.; Ma, D.; Olsen, J.; Truhlar, D. G.; Gagliardi, L. Multiconfiguration pair-density functional theory. *J. Chem. Theory Comput.* **2014**, *10*, 3669–3680.
- (50) Ghigo, G.; Roos, B. O.; Malmqvist, P.-Å. A modified definition of the zeroth-order Hamiltonian in multiconfigurational perturbation theory (CASPT2). *Chem. Phys. Lett.* **2004**, *396*, 142–149.
- (51) Kepenekian, M.; Robert, V.; Le Guennic, B. What zeroth-order Hamiltonian for CASPT2 adiabatic energetics of Fe(II)N₆ architectures? *J. Chem. Phys.* **2009**, *131*, 114702.
- (52) Lawson Daku, L. M.; Aquilante, F.; Robinson, T. W.; Hauser, A. Accurate spin-state energetics of transition metal complexes. 1. CCSD (T), CASPT2, and DFT study of [M(NCH)₆]²⁺ (M = Fe, Co). *J. Chem. Theory Comput.* **2012**, *8*, 4216–4231.
- (53) Rintelman, J. M.; Adamovic, I.; Varganov, S.; Gordon, M. S. Multireference second-order perturbation theory: How size consistent is almost size consistent? *J. Chem. Phys.* **2005**, *122*, 044105.

Supporting Information for Efficient adiabatic connection approach for strongly correlated systems. Application to singlet-triplet gaps of biradicals

Daria Drwal,^{†,||} Pavel Beran,^{‡,¶,||} Michał Hapka,[§] Marcin Modrzejewski,[§] Adam Sokół,[†] Libor Veis,^{*,‡} and Katarzyna Pernal^{*,†}

[†]*Institute of Physics, Lodz University of Technology,
ul. Wolczanska 219, 90-924 Lodz, Poland*

[‡]*J. Heyrovský Institute of Physical Chemistry, Academy of Sciences of the Czech
Republic, v.v.i., Dolejškova 3, 18223 Prague 8, Czech Republic*

[¶]*Faculty of Mathematics and Physics, Charles University, Prague, Czech Republic*

[§]*Faculty of Chemistry, University of Warsaw, ul. L. Pasteura 1, 02-093 Warsaw, Poland*

^{||}*Contributed equally.*

E-mail: libor.veis@jh-inst.cas.cz; pernak@gmail.com

Coupling-constant-dependent ERPA matrices

For a given reference wavefunction Ψ^{ref} , introduce spin-free 1- and 2-RDMs, γ and Γ , respectively, as

$$\gamma_{pq} = \langle \Psi^{\text{ref}} | \hat{a}_{q\alpha}^\dagger \hat{a}_{p\alpha} | \Psi^{\text{ref}} \rangle + \langle \Psi^{\text{ref}} | \hat{a}_{q\beta}^\dagger \hat{a}_{p\beta} | \Psi^{\text{ref}} \rangle \quad (1)$$

and

$$\begin{aligned}
2\Gamma_{pqrs} = & \langle \Psi^{\text{ref}} | \hat{a}_{r\alpha}^\dagger \hat{a}_{s\alpha}^\dagger \hat{a}_{q\alpha} \hat{a}_{p\alpha} | \Psi^{\text{ref}} \rangle + \langle \Psi^{\text{ref}} | \hat{a}_{r\alpha}^\dagger \hat{a}_{s\beta}^\dagger \hat{a}_{q\beta} \hat{a}_{p\alpha} | \Psi^{\text{ref}} \rangle \\
& + \langle \Psi^{\text{ref}} | \hat{a}_{r\beta}^\dagger \hat{a}_{s\beta}^\dagger \hat{a}_{q\beta} \hat{a}_{p\beta} | \Psi^{\text{ref}} \rangle + \langle \Psi^{\text{ref}} | \hat{a}_{r\beta}^\dagger \hat{a}_{s\alpha}^\dagger \hat{a}_{q\alpha} \hat{a}_{p\beta} | \Psi^{\text{ref}} \rangle .
\end{aligned} \tag{2}$$

Using the representation of the natural orbitals

$$\gamma_{pq} = 2 \delta_{pq} n_p \tag{3}$$

(notice that $\forall_p 0 \leq n_p \leq 1$) the spin-free ERPA matrices

$$\mathcal{A}_+^\alpha = \mathcal{N}^{-1/2} (\mathcal{A}^\alpha + \mathcal{B}^\alpha) \mathcal{N}^{-1/2} \tag{4}$$

$$\mathcal{A}_-^\alpha = \mathcal{N}^{-1/2} (\mathcal{A}^\alpha - \mathcal{B}^\alpha) \mathcal{N}^{-1/2} \tag{5}$$

$$\forall_{\substack{p>q \\ r>s}} \mathcal{N}_{pq,rs} = \delta_{pr} \delta_{qs} (n_p - n_q) \tag{6}$$

are given explicitly in terms of 1- and 2-RDMs and the pertinent expression reads

$$\begin{aligned}
\forall_{pqrs} [\mathcal{A}^\alpha]_{pq,rs} = & [\mathcal{B}^\alpha]_{pq,rs} \\
= & h_{sq}^\alpha \delta_{pr} (n_p - n_s) + h_{pr}^\alpha \delta_{sq} (n_q - n_r) \\
& + \sum_{tu} \langle st | \widetilde{qu} \rangle_\alpha \Gamma_{purt} + \sum_{tu} \langle st | \widetilde{uq} \rangle_\alpha \Gamma_{putr} \\
& + \sum_{tu} \langle up | \widetilde{tr} \rangle_\alpha \Gamma_{stqu} + \sum_{tu} \langle up | \widetilde{rt} \rangle_\alpha \Gamma_{stqu} \\
& - \sum_{tu} \langle ps | \widetilde{tu} \rangle_\alpha \Gamma_{tuqr} - \sum_{tu} \langle tu | \widetilde{qr} \rangle_\alpha \Gamma_{sput} \\
& - \frac{1}{2} \delta_{sq} \sum_{twu} \langle tp | \widetilde{wu} \rangle_\alpha \Gamma_{wutr} - \frac{1}{2} \delta_{sq} \sum_{twu} \langle tp | \widetilde{uw} \rangle_\alpha \Gamma_{wurt} \\
& - \frac{1}{2} \delta_{pr} \sum_{tuw} \langle tu | \widetilde{wq} \rangle_\alpha \Gamma_{swut} - \frac{1}{2} \delta_{pr} \sum_{tuw} \langle tu | \widetilde{qw} \rangle_\alpha \Gamma_{swtu} .
\end{aligned} \tag{7}$$

The coupling-constant-dependent modified one- and two-electron integrals are defined as

$$h_{pq}^\alpha = \alpha h_{pq} + \delta_{I_p I_q} (1 - \alpha) h_{pq}^{\text{eff}} \quad , \quad (8)$$

$$h_{pq}^{\text{eff}} = h_{pq} + \sum_{J \neq I} \sum_{r \in J} n_r [2 \langle pr | qr \rangle - \langle pr | rq \rangle] \quad . \quad (9)$$

$$\langle \widetilde{pq} | rs \rangle_\alpha = [\alpha + \delta_{I_r I_s} \delta_{I_s I_p} \delta_{I_p I_q} (1 - \alpha)] \langle pq | rs \rangle \quad , \quad (10)$$

the symbol $\delta_{I_p I_q}$ stands for 1 if orbitals p and q are from the same orbital group (both are inactive, occupied or virtual) and 0 otherwise.

The matrices $\mathcal{A}_\pm^{(0)}$ and $\mathcal{A}_\pm^{(1)}$ needed to find the AC correlation energy using the iterative scheme and the Cholesky decomposition, see Eqs.(35)-(39) in the main text, follow immediately from Eqs.(4), (5), namely

$$\mathcal{A}_\pm^{(0)} = \mathcal{A}^{(0)} \pm \mathcal{B}^{(0)} \quad , \quad (11)$$

$$\mathcal{A}_\pm^{(1)} = \mathcal{A}^{(1)} \pm \mathcal{B}^{(1)} \quad , \quad (12)$$

where the matrices $\mathcal{A}^{(0)}$, $\mathcal{B}^{(0)}$ are obtained from Eq.(7) by replacing h_{pq}^α and $\langle \widetilde{pq} | rs \rangle_\alpha$ integrals with their zero-order counterparts $h_{pq}^{(0)}$, $\langle \widetilde{pq} | rs \rangle^{(0)}$ reading

$$h_{pq}^{(0)} = \delta_{I_p I_q} h_{pq}^{\text{eff}} \quad , \quad (13)$$

$$\langle \widetilde{pq} | rs \rangle^{(0)} = \delta_{I_r I_s} \delta_{I_s I_p} \delta_{I_p I_q} \langle pq | rs \rangle \quad . \quad (14)$$

Similarly, first-order matrices $\mathcal{A}^{(1)}$, $\mathcal{B}^{(1)}$ follow from Eq.(7) if the elements

$$h_{pq}^{(1)} = \alpha h_{pq} - \delta_{I_p I_q} h_{pq}^{\text{eff}} \quad , \quad (15)$$

$$\langle \widetilde{pq} | rs \rangle^{(1)} = (1 - \delta_{I_r I_s} \delta_{I_s I_p} \delta_{I_p I_q}) \langle pq | rs \rangle \quad . \quad (16)$$

replace h_{pq}^α and $\langle \widetilde{pq} | rs \rangle_\alpha$, respectively.

Frequency-dependent density-density linear response function in the ERPA approximation

Begin with the coupling-constant dependent ERPA problem

$$\begin{pmatrix} \mathcal{A}_-^\alpha & 0 \\ 0 & \mathcal{A}_+^\alpha \end{pmatrix} \begin{pmatrix} \tilde{\mathbf{Y}}_\nu^\alpha \\ \tilde{\mathbf{X}}_\nu^\alpha \end{pmatrix} = \omega_\nu^\alpha \begin{pmatrix} \mathbf{0} & \mathbf{1} \\ \mathbf{1} & \mathbf{0} \end{pmatrix} \begin{pmatrix} \tilde{\mathbf{Y}}_\nu^\alpha \\ \tilde{\mathbf{X}}_\nu^\alpha \end{pmatrix}, \quad (17)$$

where the eigenvectors are orthonormal in the following sense

$$\forall_{\mu,\nu} \quad 2\tilde{\mathbf{Y}}_\mu^\alpha \tilde{\mathbf{X}}_\nu^\alpha = \delta_{\mu\nu} \quad (18)$$

The matrices \mathcal{A}_\pm^α , defined in Eqs.(4)-(7), are assumed to be positive definite. This condition is met if the reference wavefunction satisfies the Hellman-Feynman theorem, since in such a case the EPRA matrices are equivalent to the Hessian matrix describing variations of energy with respect to orbital rotations. It can be shown [see theorem A.5 in Furche, JCP 114, 5982 (2001)] that spectral decomposition of the matrices \mathcal{A}_\pm^α is given by eigenvalues and eigenvectors

$$\bar{\mathbf{X}}_\nu^\alpha = \sqrt{2}\tilde{\mathbf{X}}_\nu^\alpha \quad (19)$$

$$\bar{\mathbf{Y}}_\nu^\alpha = \sqrt{2}\tilde{\mathbf{Y}}_\nu^\alpha \quad (20)$$

orthonormal in the following sense

$$\forall_{\mu,\nu} \quad \bar{\mathbf{Y}}_\mu^\alpha \bar{\mathbf{X}}_\nu^\alpha = \delta_{\mu\nu} \quad (21)$$

as

$$\mathcal{A}_+^\alpha = \begin{pmatrix} \bar{\mathbf{Y}}_1^\alpha & \bar{\mathbf{Y}}_2^\alpha & \cdots \end{pmatrix} \begin{pmatrix} \omega_1^\alpha & 0 & \cdots \\ 0 & \omega_2^\alpha & \cdots \\ \cdots & \cdots & \cdots \end{pmatrix} \begin{pmatrix} [\bar{\mathbf{Y}}_1^\alpha]^\text{T} \\ [\bar{\mathbf{Y}}_2^\alpha]^\text{T} \\ \cdots \end{pmatrix} \quad (22)$$

and

$$\mathcal{A}_-^\alpha = \begin{pmatrix} \bar{\mathbf{X}}_1^\alpha & \bar{\mathbf{X}}_2^\alpha & \cdots \end{pmatrix} \begin{pmatrix} \omega_1^\alpha & 0 & \cdots \\ 0 & \omega_2^\alpha & \cdots \\ \cdots & \cdots & \cdots \end{pmatrix} \begin{pmatrix} [\bar{\mathbf{X}}_1^\alpha]^\text{T} \\ [\bar{\mathbf{X}}_2^\alpha]^\text{T} \\ \cdots \end{pmatrix} . \quad (23)$$

Using the orthonormality condition, Eq.(21), and Eqs.(19)-(20), it can be checked by inspection that a matrix $\mathbf{C}^\alpha(\omega)$ satisfying the following equation

$$[\mathcal{A}_+^\alpha \mathcal{A}_-^\alpha + \omega^2 \mathbf{1}] \mathbf{C}^\alpha(\omega) = \mathcal{A}_+^\alpha \quad (24)$$

is the dynamic linear response function, see Eq.(21) in the main text,

$$\forall_{\substack{p>q \\ r>s}} C_{pq,rs}^\alpha(\omega) = 2 \sum_\nu \left[\tilde{\mathbf{Y}}_\nu^\alpha \right]_{pq} \frac{\omega_\nu}{(\omega_\nu)^2 + \omega^2} \left[\tilde{\mathbf{Y}}_\nu^\alpha \right]_{rs} . \quad (25)$$

Table 1: Convergence check for biradicals molecules. Energies in [Ha], ST gaps (differences between triplet and singlet energies) in [eV]. Systems (Sys.): 1 – C_4H_4 , 2 – $C_5H_5^+$, 3 – $C_4H_3NH_2$, 4 – C_4H_3CHO , 5 – $C_4H_2NH_2(CHO)$, 6 – $C_4H_2-1,2-(CH_2)_2$, 7 – $C_4H_2-1,3-(CH_2)_2$, 8 – divergent case of $C_5H_5^+$ and CAS(2,4).

Sys.	n	AC _n (S)	AC _n (T)	AC _n (S)-AC(S)	AC _n (T)-AC(T)	AC _n (ST)	AC _n (ST)-AC(ST)
1	1	-154.38675	-154.38681	-0.01993	-0.02478	-0.00144	-0.13201
	2	-154.35211	-154.36192	0.01471	0.00011	-0.26684	-0.39741
	3	-154.37064	-154.36790	-0.00381	-0.00587	0.07450	-0.05607
	4	-154.36520	-154.35905	0.00162	0.00297	0.16744	0.03687
	5	-154.36751	-154.36354	-0.00069	-0.00151	0.10811	-0.02246
	7	-154.36697	-154.36251	-0.00015	-0.00049	0.12129	-0.00928
	10	-154.36681	-154.36192	0.00001	0.00011	0.13320	0.00263
	12	-154.36682	-154.36198	0.00000	0.00004	0.13174	0.00117
	15	-154.36683	-154.36204	0.00000	-0.00002	0.13021	-0.00036
	AC	-154.36682	-154.36202	-	-	0.13057	-
2	1	-192.78598	-192.81767	-0.02010	-0.02386	-0.86239	-0.10249
	2	-192.74597	-192.77359	0.01992	0.02022	-0.75165	0.00824
	3	-192.77033	-192.79950	-0.00444	-0.00569	-0.79389	-0.03400
	4	-192.76255	-192.79086	0.00333	0.00295	-0.77025	-0.01035
	5	-192.76682	-192.79519	-0.00094	-0.00139	-0.77207	-0.01217
	7	-192.76610	-192.79422	-0.00022	-0.00041	-0.76512	-0.00523
	10	-192.76553	-192.79372	0.00035	0.00009	-0.76691	-0.00702
	12	-192.76565	-192.79377	0.00023	0.00004	-0.76510	-0.00521
	15	-192.76586	-192.79381	0.00003	0.00000	-0.76059	-0.00069
	AC	-192.76588	-192.79381	-	-	-0.75989	-
3	1	-209.68148	-209.68454	-0.03926	-0.04462	-0.08319	-0.14584
	2	-209.61974	-209.61310	0.02248	0.02682	0.18065	0.11800

Sys.	n	AC _n (S)	AC _n (T)	AC _n (S)-AC(S)	AC _n (T)-AC(T)	AC _n (ST)	AC _n (ST)-AC(ST)
	3	-209.64932	-209.64934	-0.00709	-0.00942	-0.00061	-0.06326
	4	-209.63933	-209.63531	0.00289	0.00461	0.10950	0.04685
	5	-209.64365	-209.64235	-0.00142	-0.00243	0.03523	-0.02742
	7	-209.64256	-209.64071	-0.00033	-0.00079	0.05023	-0.01242
	10	-209.64216	-209.63970	0.00006	0.00022	0.06702	0.00437
	12	-209.64219	-209.63981	0.00003	0.00011	0.06479	0.00214
	15	-209.64220	-209.63993	0.00002	0.00000	0.06193	-0.00072
	AC	-209.64222	-209.63992	-	-	0.06265	-
	1	-267.57835	-267.57912	-0.06117	-0.06606	-0.02111	-0.13292
	2	-267.48330	-267.47536	0.03387	0.03771	0.21615	0.10434
	3	-267.53097	-267.52893	-0.01379	-0.01587	0.05536	-0.05646
	4	-267.51019	-267.50456	0.00699	0.00851	0.15309	0.04128
4	5	-267.52136	-267.51816	-0.00418	-0.00509	0.08705	-0.02476
	7	-267.51880	-267.51512	-0.00162	-0.00205	0.09996	-0.01185
	10	-267.51662	-267.51233	0.00056	0.00074	0.11661	0.00480
	12	-267.51686	-267.51265	0.00032	0.00042	0.11454	0.00273
	15	-267.51724	-267.51318	-0.00006	-0.00011	0.11055	-0.00126
	AC	-267.51718	-267.51307	-	-	0.11181	-
	1	-322.88405	-322.87894	-0.07863	-0.08765	0.13894	-0.24570
	2	-322.75998	-322.74413	0.04545	0.04716	0.43122	0.04658
	3	-322.82401	-322.81120	-0.01858	-0.01991	0.34854	-0.03610
	4	-322.79486	-322.78070	0.01057	0.01059	0.38516	0.00052
	5	-322.81221	-322.79752	-0.00679	-0.00624	0.39960	0.01496
5	7	-322.80884	-322.79377	-0.00341	-0.00248	0.41001	0.02537
	10	-322.80384	-322.79036	0.00159	0.00093	0.36678	-0.01786
	12	-322.80431	-322.79075	0.00111	0.00054	0.36910	-0.01553

Sys.	n	AC _n (S)	AC _n (T)	AC _n (S)-AC(S)	AC _n (T)-AC(T)	AC _n (ST)	AC _n (ST)-AC(ST)
	15	-322.80606	-322.79141	-0.00064	-0.00012	0.39881	0.01417
	AC	-322.80542	-322.79129	-	-	0.38464	-
6	1	-231.74407	-231.61704	-0.03381	-0.03307	3.45658	0.02014
	2	-231.68434	-231.56013	0.02591	0.02384	3.38011	-0.05632
	3	-231.71815	-231.59113	-0.00790	-0.00716	3.45641	0.01998
	4	-231.70636	-231.58071	0.00389	0.00326	3.41918	-0.01725
	5	-231.71231	-231.58559	-0.00206	-0.00163	3.44816	0.01173
	7	-231.71092	-231.58440	-0.00067	-0.00043	3.44276	0.00632
	10	-231.71012	-231.58386	0.00014	0.00011	3.43570	-0.00074
	12	-231.71018	-231.58390	0.00007	0.00007	3.43621	-0.00022
	15	-231.71024	-231.58394	0.00001	0.00003	3.43697	0.00054
		AC	-231.71026	-231.58397	-	-	3.43643
7	1	-231.64530	-231.67913	-0.03302	-0.03372	-0.92055	-0.01902
	2	-231.58760	-231.62092	0.02469	0.02450	-0.90673	-0.00520
	3	-231.61972	-231.65290	-0.00744	-0.00749	-0.90286	-0.00133
	4	-231.60880	-231.64197	0.00348	0.00344	-0.90265	-0.00112
	5	-231.61416	-231.64717	-0.00187	-0.00176	-0.89839	0.00314
	7	-231.61288	-231.64591	-0.00060	-0.00049	-0.89866	0.00288
	10	-231.61219	-231.64531	0.00010	0.00011	-0.90132	0.00021
	12	-231.61224	-231.64536	0.00005	0.00006	-0.90128	0.00025
	15	-231.61228	-231.64540	0.00000	0.00002	-0.90104	0.00050
		AC	-231.61228	-231.64541	-	-	-0.90153
	1	-192.79829	-192.82560	-0.04506	-0.03862	-0.74314	0.17552
	2	-192.72167	-192.75934	0.03156	0.02764	-1.02505	-0.10639
	3	-192.77238	-192.79638	-0.01916	-0.00940	-0.65307	0.26559

Sys.	n	$AC_n(S)$	$AC_n(T)$	$AC_n(S)-AC(S)$	$AC_n(T)-AC(T)$	$AC_n(ST)$	$AC_n(ST)-AC(ST)$
	4	-192.74718	-192.78110	0.00605	0.00589	-0.92301	-0.00435
	5	-192.76827	-192.78992	-0.01505	-0.00294	-0.58913	0.32953
	6	-192.75531	-192.78477	-0.00208	0.00222	-0.80165	0.11701
	7	-192.77100	-192.78820	-0.01778	-0.00121	-0.46776	0.45090
	8	-192.76309	-192.78593	-0.00986	0.00106	-0.62151	0.29715
	9	-192.77912	-192.78757	-0.02589	-0.00058	-0.23021	0.68845
	10	-192.77532	-192.78642	-0.02209	0.00057	-0.30205	0.61661
AC		-192.75323	-192.78699	-	-	-0.91866	-

Timings

Table 2 shows timings for AC, AC_n and AC0 correlation energy calculations for singlet energy of C₄H₂-1,3-(CH₂)₂ biradical in two basis sets: aug-cc-pVTZ (aTZ) and aug-cc-pVQZ (aQZ).

Table 2: CPU times of computing correlation energy for C₄H₂-1,3-(CH₂)₂ in two basis sets: aug-cc-pVTZ (aTZ) and aug-cc-pVQZ (aQZ). AC_n corresponds to n=10. The timings were measured on a 4 core Intel(R) Xeon(R) Gold 6240 CPU machine clocked at 2.60 GHz using a threaded MKL BLAS library.

	AC		AC _n		AC0	
active space	aTZ	aQZ	aTZ	aQZ	aTZ	aQZ
(4,4)	3h 14m 3s	19h 55m 18s	42m 9s	4h 1m 17s	22s	1m 26s
(6,6)	3h 54m 36s	21h 38m 33s	46m 46s	4h 9m 57s	28s	1m 36s
(8,8)	3h 56m 39s	24h 52m 45s	50m 15s	4h 28m 1s	37s	2m 22s

DMRG single-orbital entropies and mutual information for selected biradicals

For all studied biradicals we have used geometries from Ref. ? and aug-cc-pVTZ basis set. ? For the representative examples of C_4H_4 and $C_5H_5^+$ we have performed the CASSCF orbital optimizations in the medium size active spaces of Ref. ? (mCPO). Moreover, for C_4H_4 we have also performed DMRG-SCF optimizations in eCPO with fixed bond dimensions $M = 2000$, i.e. CAS(20,22), to verify that there is essentially no difference between correlations in mCPO and eCPO. In other words, the additional orbitals not included in mCPO are only weakly correlated. Finally, we have computed the DMRG($M_{\max} = 4000$) single-orbital entropies (s_i), as well as mutual information (I_{ij}), ? which provide additional information on the correlation structure.

The DMRG single-orbital entropies for C_4H_4 (eCPO, mCPO) and $C_5H_5^+$ (mCPO) are shown in Figures 1 - 3.

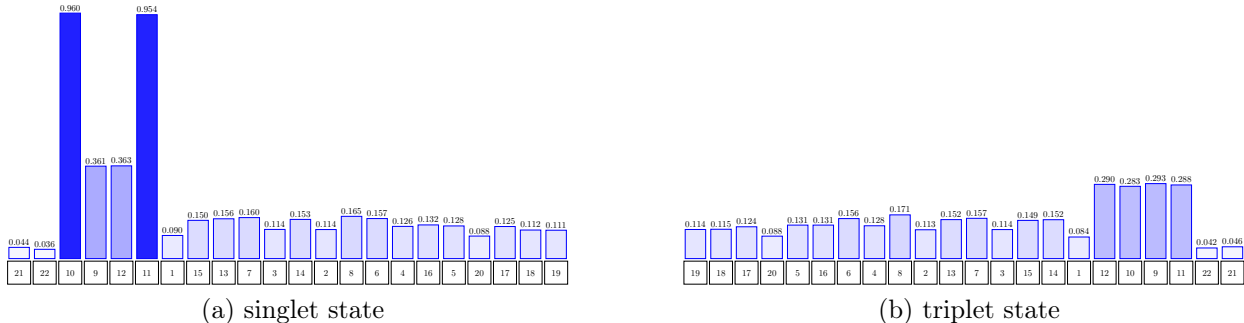


Figure 1: The DMRG single-orbital entropies for C_4H_4 and eCPO, i.e. CAS(20,22). The orbital indices correspond to the ordering from Figures 4 and 5.

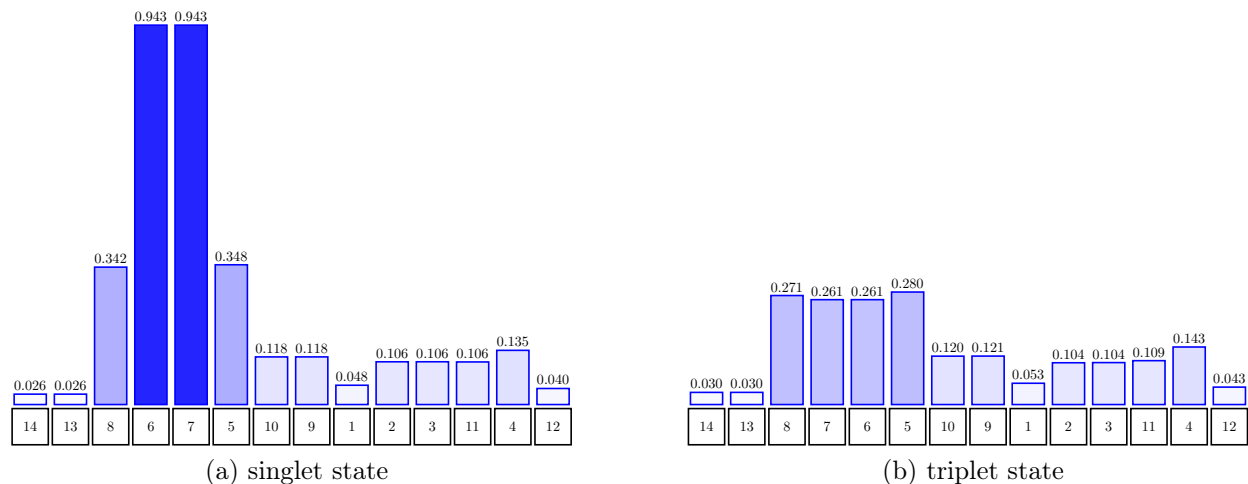


Figure 2: The DMRG single-orbital entropies for C_4H_4 and mCPO, i.e. CAS(12,14). The orbital indices correspond to the ordering from Figures 6 and 7.

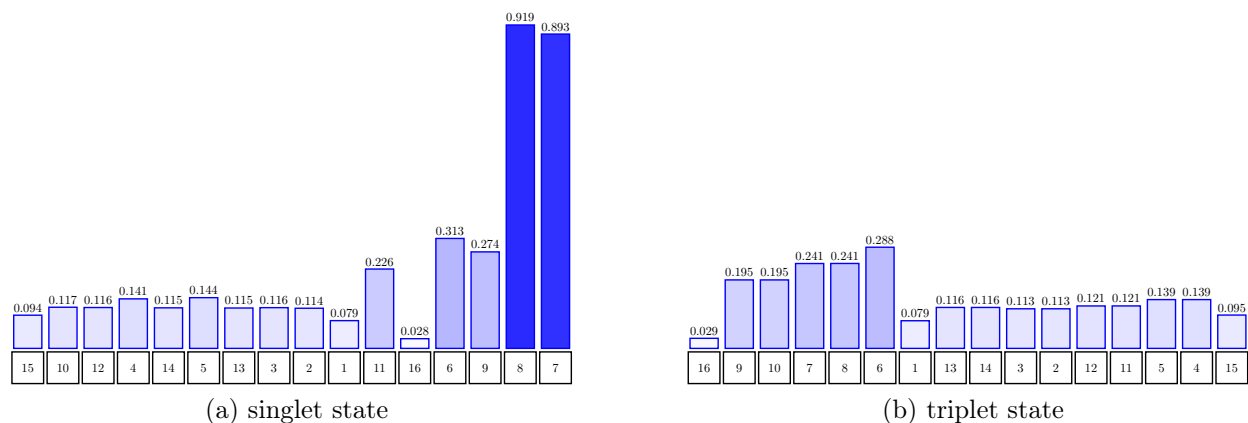


Figure 3: The DMRG single-orbital entropies for $C_5H_5^+$ and mCPO, i.e. CAS(14,16). The orbital indices correspond to the ordering from Figures 8 and 9.

CASSCF natural orbitals for selected biradicals

The DMRG-SCF (C_4H_4 , eCPO) natural orbitals with their occupation numbers are depicted in Figures 4 and 5. CASSCF (C_4H_4 , $C_5H_5^+$, mCPO) natural orbitals and the corresponding occupation numbers are depicted in Figures 6, 7, 8, and 9.

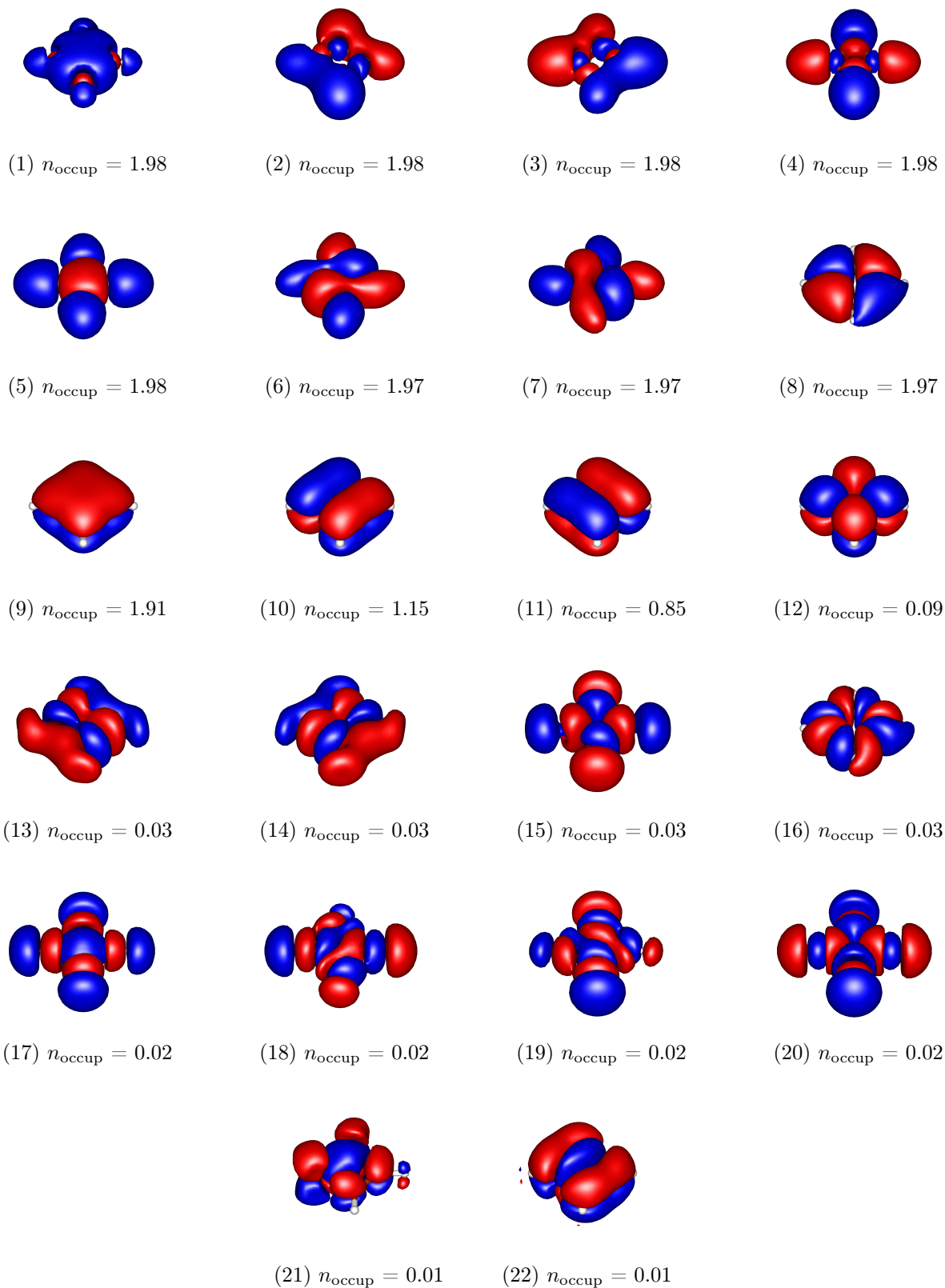


Figure 4: C_4H_4 , singlet state, DMRG-SCF(20, 22)

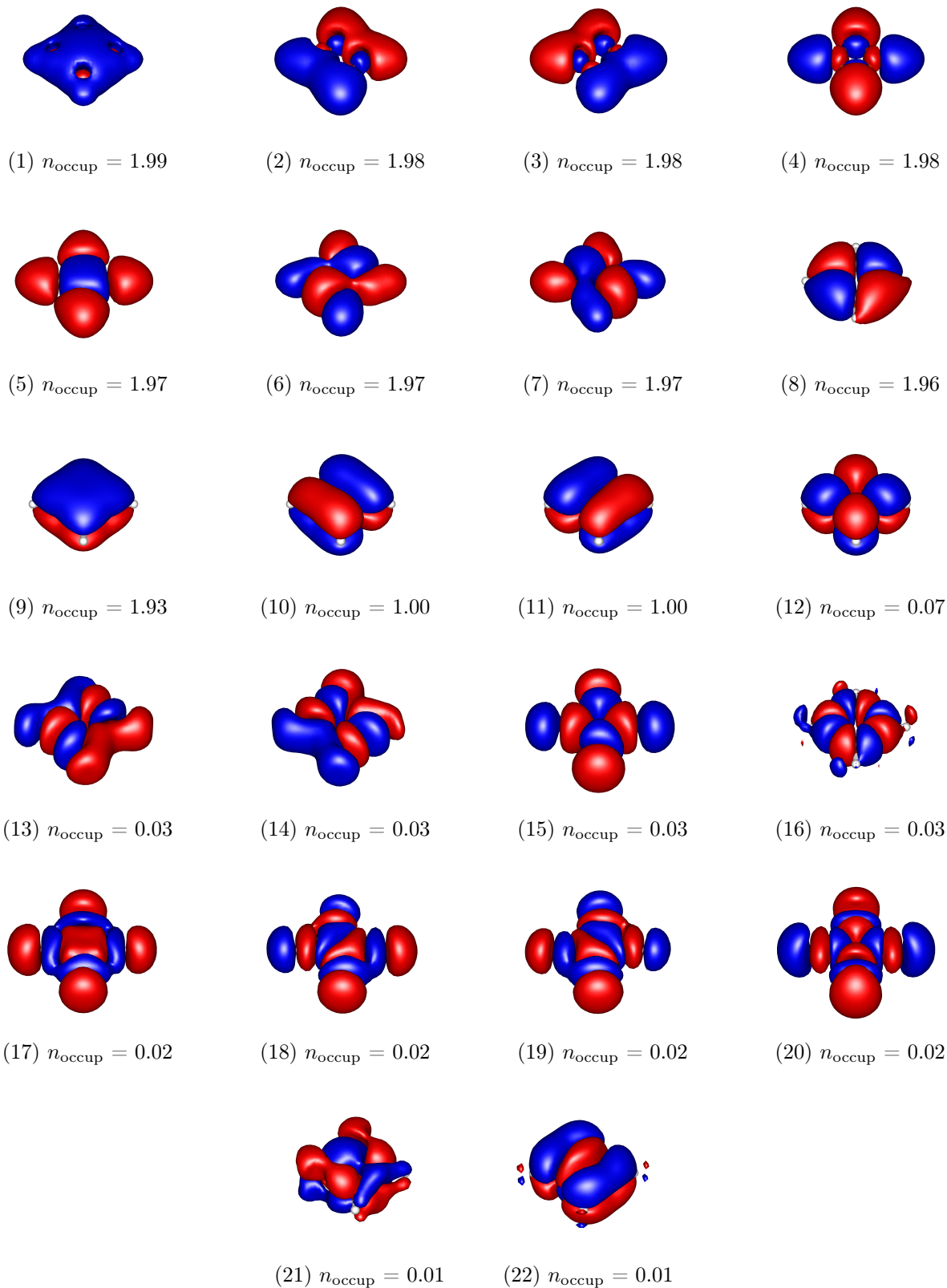


Figure 5: C_4H_4 , triplet state, DMRG-SCF(20, 22)

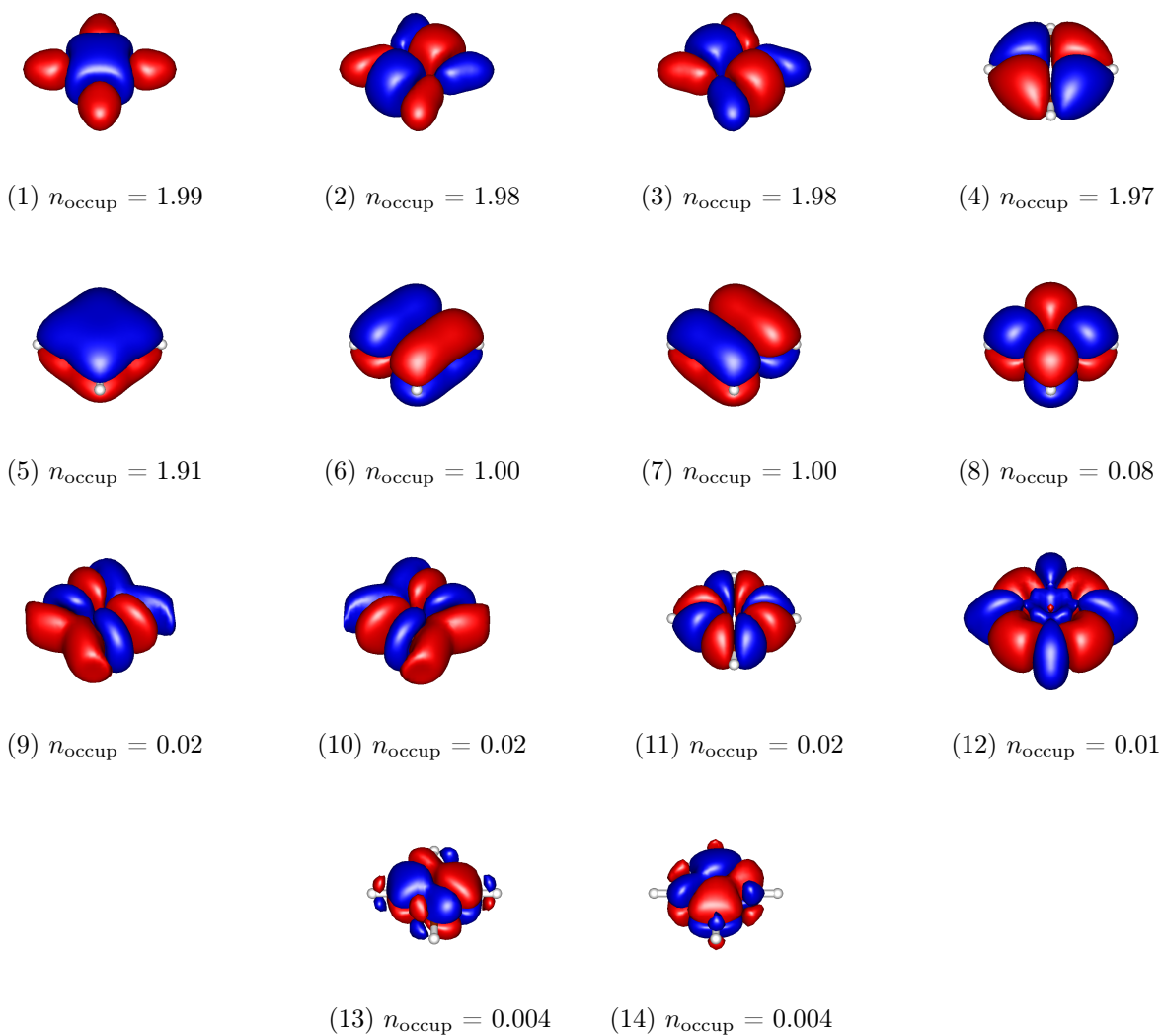


Figure 6: C_4H_4 , singlet state, CASSCF(12, 14)

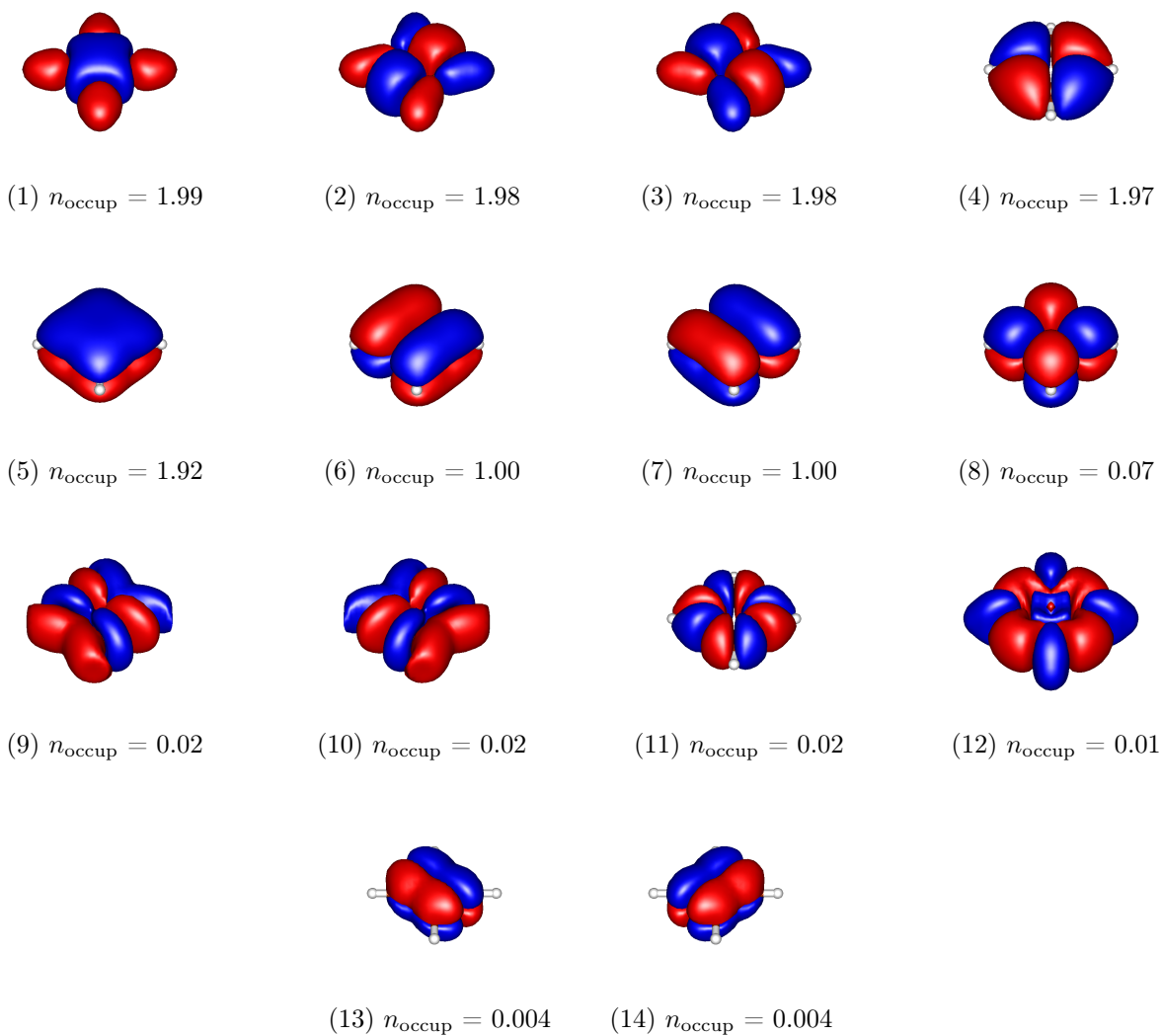


Figure 7: C_4H_4 , triplet state, CASSCF(12, 14)

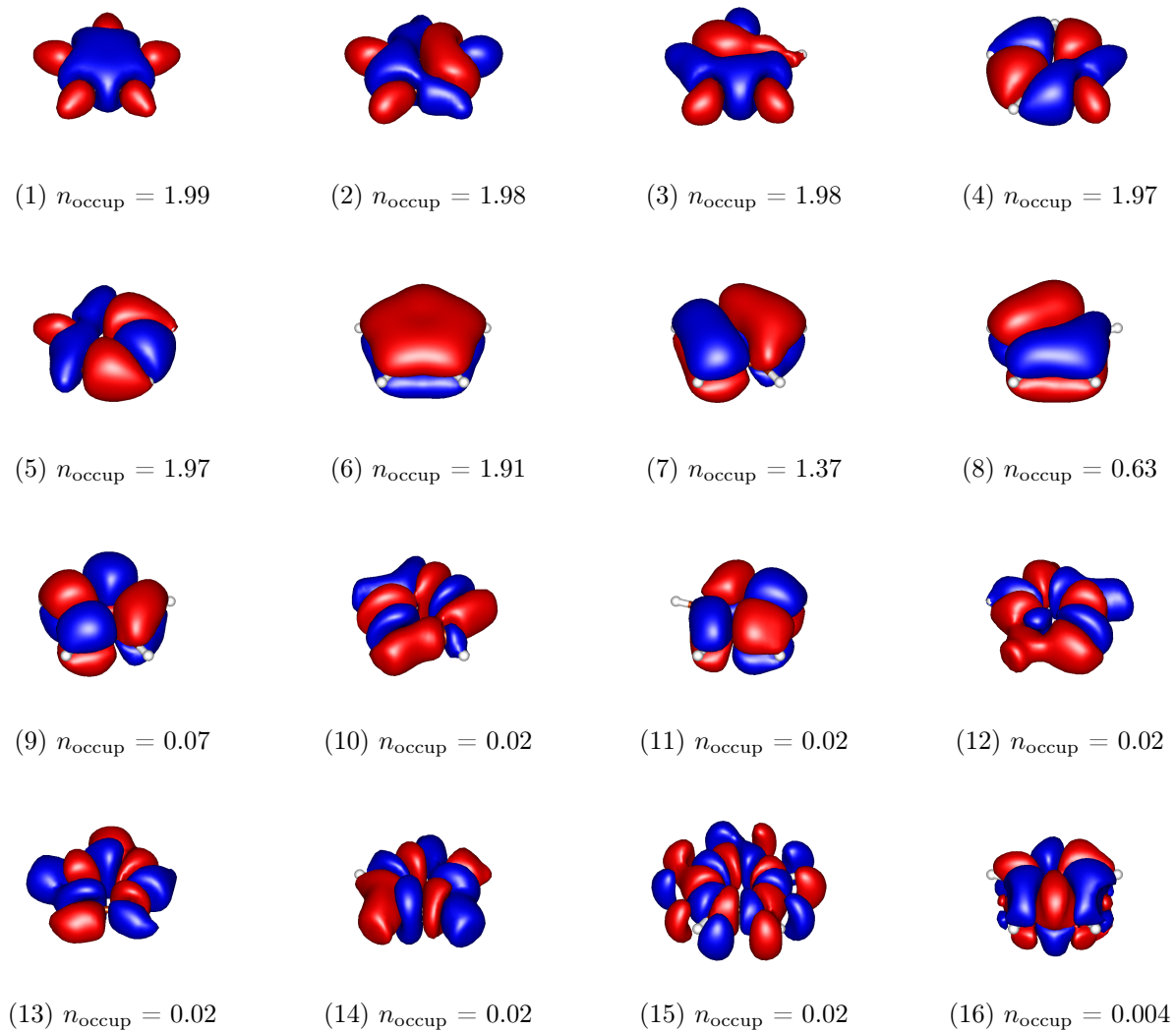


Figure 8: C_5H_5 , singlet state, CASSCF(14, 16)

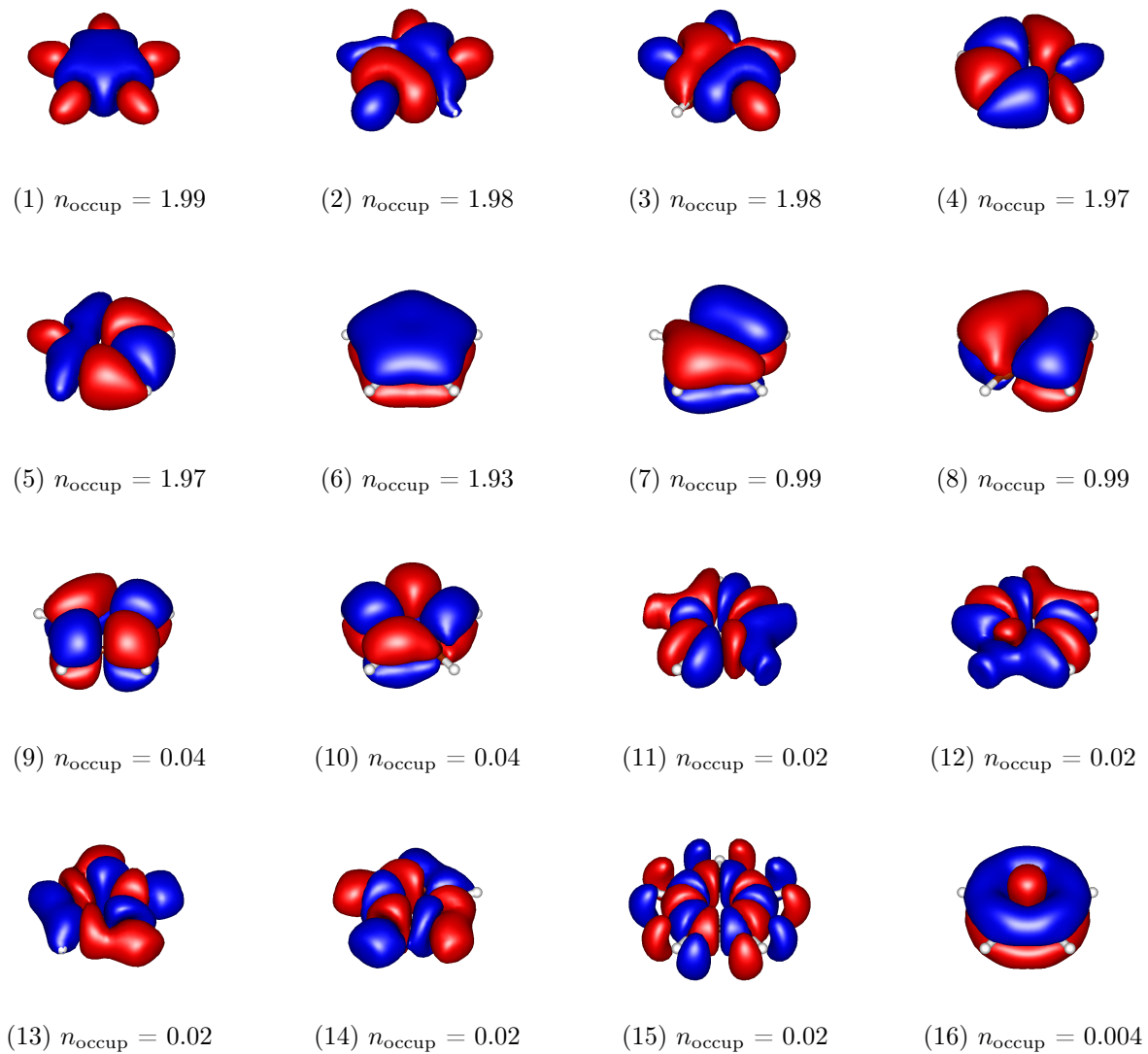


Figure 9: C_5H_5 , triplet state, CASSCF(14, 16)